



# Isoprene derived secondary organic aerosol in a global aerosol chemistry climate model

Scarlet Stadtler<sup>1</sup>, Thomas Kühn<sup>2,3</sup>, Sabine Schröder<sup>1</sup>, Domenico Taraborrelli<sup>1</sup>, Martin G. Schultz<sup>1,\*</sup>, and Harri Kokkola<sup>2</sup>

<sup>1</sup>Institut für Energie- und Klimaforschung, IEK-8, Forschungszentrum Jülich, Germany

<sup>2</sup>Finnish Meteorological Institute, P.O. Box 1627, 70211, Kuopio, Finland

<sup>3</sup>Department of Applied Physics, University of Eastern Finland, P.O. Box 1627, 70211, Kuopio, Finland

\*Now at Jülich Supercomputing Centre, JSC, Forschungszentrum Jülich, Germany

Correspondence to: Harri Kokkola ([harri.kokkola@fmi.fi](mailto:harri.kokkola@fmi.fi))

## Abstract

Within the framework of the global chemistry climate model ECHAM-HAMMOZ a novel explicit coupling between the sectional aerosol model HAM-SALSA and the chemistry model MOZ was established to form isoprene derived secondary organic aerosol (iSOA). Isoprene oxidation in the chemistry model MOZ is described by a semi-explicit scheme consisting of 147 reactions, embedded in a detailed atmospheric chemical mechanism with a total of 779 reactions. Low volatile compounds (LVOC) produced during isoprene photooxidation are identified and explicitly partitioned by HAM-SALSA. A group contribution method was used to estimate their evaporation enthalpies and corresponding saturation vapor pressures, which are used by HAM-SALSA to calculate the saturation concentration of each LVOC. With this method, every single precursor is tracked in terms of condensation and evaporation in each aerosol size bin. This approach lead to the identification of ISOP(OOH)<sub>2</sub> as a main contributor to iSOA formation. Further, reactive uptake of isoprene epoxidiols (IEPOX) and isoprene derived glyoxal were included as iSOA sources. The parameterization of IEPOX reactive uptake includes a dependency on aerosol pH value. This model framework connecting semi-explicit isoprene oxidation with explicit treatment of aerosol tracers leads to a global, annual isoprene SOA yield of 16% relative to the primary oxidation of isoprene by OH, NO<sub>3</sub>, and ozone. With 445 Tg (392 TgC) isoprene emitted, an iSOA source of 148 Tg (61 TgC) is simulated. The major part of iSOA in ECHAM-HAMMOZ is produced by IEPOX (24.4 TgC) and ISOP(OOH)<sub>2</sub> (28.3 TgC). The main sink process is particle wet deposition which removes 143 Tg (59 TgC). The iSOA burden reaches 1.6 Tg (0.7 TgC) in the year 2012.

## 1 Introduction

Atmospheric particles play an important role in the earth system, especially in the interactions between climate (IPCC, 2013) and human health (Fröhlich-Nowoisky et al., 2016; Lakey et al., 2016). Aerosols interact with atmospheric radiation directly via absorption and scattering, and indirectly via cloud formation. These interactions depend on the particles' microphysical



properties, their chemical composition and phase state (Ghan and Schwartz, 2007; Shiraiwa et al., 2017). In the current political debates about air quality and climate change, understanding atmospheric particles is one of the most challenging problems and led to increased research in this field over the last two decades (Fuzzi et al., 2015). Especially organic aerosols are not well understood and subject of ongoing research (Pandis et al., 1992; Kanakidou et al., 2005; Zhang et al., 2007; Fuzzi et al., 2015; 5 Hodzic et al., 2016). Organic aerosol (OA) consists of two types of particles, often mixed and difficult to distinguish (Kavouras et al., 1999; Donahue et al., 2009). First, organic aerosol can be emitted directly into the atmosphere as primary organic aerosol (POA) (Kanakidou et al., 2005; Dentener et al., 2006). Second, organic aerosol mass is also formed from organic gases which are emitted as volatile organic compounds (VOC) and transformed into compounds capable of partitioning into the particle phase. This second type of organic aerosol is called secondary organic aerosol (SOA) (Pankow, 1994; Seinfeld and Pankow, 10 2003; Jimenez et al., 2009). Both types of organic aerosols are challenging to model due to limited knowledge about emissions, composition, evolution and physicochemical properties (Lin et al., 2012). Concerning SOA, there are additional uncertainties concerning SOA precursors and the atmospheric chemistry leading to their formation (Heald et al., 2005). Up to now, global models have lacked an explicit treatment of SOA (Zhang et al., 2007) and use relatively simple parameterisations to form SOA, for example with the two-product model based on Odum et al. (1996). Such parameterisations neglect explicit chemical 15 transformation and assume fixed SOA yields based on laboratory studies (Tsigaridis and Kanakidou, 2003; O'Donnell et al., 2011). Donahue et al. (2006) presented with their volatility basis set (VBS) another approach that allows to distinguish between various precursor VOC, but still does not consider explicit chemical formation and molecular identity of the compounds. The VBS system was further developed to include aerosol aging based on observations of O:C ratio (Donahue et al., 2011). Lin et al. (2012) and Marais et al. (2016) made first steps into coupling explicit formation of SOA precursors with SOA formation, 20 focusing on specific compounds.

Global models largely underestimate the amount of atmospheric organic aerosol (Volkamer et al., 2006; De Gouw and Jimenez, 2009; Tsigaridis et al., 2014). This underestimation might be related to the huge number of organic compounds in the atmosphere (Goldstein and Galbally, 2007) which cannot be identified individually by state-of-the-art measuring devices. For explicit modeling it is necessary to characterize their chemical properties, structures, volatility, solubility and further 25 reactions pathways in the particle phase. Donahue et al. (2009) argues that it is extremely difficult to accomplish dissecting this complexity in detail.

This study makes an attempt to explore the influence of a semi-explicit chemical mechanism implementing a state-of-the-art isoprene oxidation that is based on Taraborrelli et al. (2009, 2012); Nölscher et al. (2014); Lelieveld et al. (2016) on isoprene derived secondary organic aerosol (iSOA) formation. Recently, isoprene was identified to contribute to SOA. Literature iSOA 30 yields vary between 1% and 30% relative to the total amount of isoprene oxidized by OH, O<sub>3</sub>, and NO<sub>3</sub> (Surratt et al., 2010). Even with a yield as low as 1%, isoprene as a source of SOA has a huge impact, since global annual isoprene emissions are estimated to range between 500 and 750 Tg a<sup>-1</sup> (Guenther et al., 2006). Therefore, iSOA was investigated in field and laboratory experiments (Claeys et al., 2004; Surratt et al., 2006, 2007a, b). These studies could identify isoprene derived compounds in the particle phase and identified possible formation pathways (Liggio et al., 2005a; Lin et al., 2013b; Berndt



et al., 2016; DAmbro et al., 2017a). First generation products of isoprene are too volatile to partition into the the aerosol phase (Kroll et al., 2006), however they contribute significantly to iSOA formation via heterogeneous and multiphase reactions.

Glyoxal and isoprene epoxide (IEPOX) were identified to undergo reactive uptake and subsequent aqueous-phase reactions (Liggio et al., 2005b; Paulot et al., 2009). Glyoxal uptake might be followed by oligomerization and organo-sulfate formation depending on aerosol pH value, which is considered to be an irreversible uptake (Liggio et al., 2005a, b). Therefore, glyoxal derived SOA was studied in different model configurations with reversible and irreversible uptake (Volkamer et al., 2007; Fu et al., 2008; Ervens and Volkamer, 2010; Washenfelder et al., 2011; Waxman et al., 2013; Li et al., 2013).

Experimental and ambient measurements found 2-methyltetrol in the particle phase, which is attributed to be formed by IEPOX (Claeys et al., 2004; Paulot et al., 2009; Surratt et al., 2006). Therefore, irreversible reactive uptake from IEPOX was proposed. Surratt et al. (2007b) studied the effect of pH value on iSOA and found organic carbon to be a function of aerosol pH which was further studied leading to the reaction mechanism for 2-methyltetrol formation from IEPOX to be an acid catalyzed ring opening reaction (Eddingsaas et al., 2010; Lin et al., 2013a) and was used to create process parametrizations (Pye et al., 2013; Riedel et al., 2015). Nevertheless, IEPOX uptake was mostly studied in experiments using sulfate aerosol seeds to explore IEPOX uptake dependence on aerosol pH, which leads to the question whether the reaction might be sulfate catalyzed instead (Surratt et al., 2007a; Xu et al., 2015). However, non-racemic mixtures of tetrols stereoisomers in the atmosphere point to a substantial biological origin (Nozière et al., 2011).

After exploring the IEPOX iSOA formation pathway, experimental studies could also identify non-IEPOX iSOA formation pathways via the highly oxidized, very low volatile isoprene product dihydroxy dihydroperoxide ( $C_5H_{12}O_6$ , ISOP(OOH)<sub>2</sub>) (Riva et al., 2016; Liu et al., 2016; Berndt et al., 2016; DAmbro et al., 2017a). This compound was identified under low  $NO_x$ , meaning  $HO_2$  dominated conditions (Berndt et al., 2016) and neutral aerosol pH (Liu et al., 2016; DAmbro et al., 2017a).

In the light of the available knowledge on iSOA formation, this study focuses on iSOA formation via reactive uptake and explicit partitioning of exclusively low volatile isoprene derived compounds. This paper is organized as follows: Section 2 describes the model framework including the sub-models ECHAM6, HAM-SALSA and MOZ. This includes a detailed description of the selection procedure for iSOA precursors and the interplay between the gas-phase oxidation of these and the SALSA aerosol scheme. Furthermore, Section 2 describes the model setup and sensitivity runs performed. Section 3 shows the simulation results of the reference run including all iSOA formation pathways, e.g. global annual budget and mean surface concentrations. Furthermore, it discusses sensitivity runs and model uncertainties for formulation of the reactive uptake of IEPOX and the impacts of evaporation enthalpy. Section 4 discusses possible error sources according to used parametrizations and assumptions and 5 provides conclusions.

## 30 2 Method

### 2.1 Model description

For this study the aerosol chemistry climate model ECHAM-HAMMOZ in its version ECHAM6.3-HAM2.3MOZ1.0 is used (<https://redmine.hammoz.ethz.ch/projects/hammoz/wiki/Echam630-ham23-moz10>), Schultz et al. (submitted)). This model



framework consists of three coupled models. ECHAM6 is the sixth generation climate model which evolved from the European Center for Medium Range Weather Forecasts (ECMWF) developed in the Max Planck Institute for Meteorology (Stevens et al., 2013). In order to simulate climate, ECHAM6 solves the prognostic equations for vorticity, divergence, surface pressure and temperature expressed as spherical harmonics with triangular truncation (Stier et al., 2005). All tracers are transported with a semi Lagrangian scheme on a Gaussian grid (Lin and Rood, 1996). Hybrid  $\sigma$ -pressure coordinates with a pressure range from 1013 hPa to 0.01 hPa are used for vertical discretization. Aerosol tracers are simulated by the Hamburg Aerosol Model HAM with aerosol microphysics based on the Sectional Aerosol module for Large Scale Applications SALSA (Kokkola et al., 2008; Bergman et al., 2012). In addition, the chemistry model MOZ simulates atmospheric concentrations of trace gases interacting with aerosols and climate system (Stein et al., 2012). A detailed description of the HAMMOZ model system is given in Schultz et al. (submitted).

For this study SALSA is extended to partition organic trace gases simulated by MOZ between the gas and aerosol phases. Additionally, the isoprene oxidation scheme in the MOZ chemical mechanism was modified in order to model secondary organic aerosol formation. Details can be found in Sections 2.1.1 and 2.1.2.

Aerosol and trace gas emissions are taken from the ACCMIP interpolated emission inventory (Lamarque et al., 2010). Interactive gas phase emissions of VOC are simulated by MEGAN (Model of Emissions of Gases and Aerosols from Nature) (Guenther et al., 2006). For details about the implementation of MEGAN v2.1 in ECHAM-HAMMOZ and its evaluation it is referred to Henrot et al. (2017).

For all simulations the triangular truncation 63, leading to horizontal resolution of  $1.875^\circ \times 1.875^\circ$  and 47 vertical layers is used. The lowest layer, corresponding to the surface layer, thickness is around 50 m.

### 2.1.1 Chemistry model MOZ

Atmospheric chemistry is simulated by MOZ solving the chemical equations using an implicit Euler backward solver and treating emissions, dry and wet deposition. The current MOZ version evolved from an extensive atmospheric chemical mechanism based on MOZART version 3.5 (Model for Ozone and Related chemical Tracers) (Stein et al., 2012), which merges the tropospheric version MOZART-4 (Emmons et al., 2010) with the stratospheric version MOZART-3 (Kinnison et al., 2007). The chemical mechanism was further developed including a detailed isoprene oxidation scheme based on Taraborrelli et al. (2009, 2012); Nölscher et al. (2014); Lelieveld et al. (2016) with revised peroxy radical chemistry (Schultz et al., submitted), leading to a model system resembling the CAM-chem model (Community Atmosphere Model with Chemistry) (Lamarque et al., 2010). The chemical mechanism version used here is called JAM3 (Jülich Atmospheric Mechanism version 3). It differs from version 2 of this mechanism in self and cross reactions of isoprene products, added nitrates, initial reactions for monoterpenes and sesquiterpenes and production of very low volatile highly oxidized molecules. The additional isoprene related reactions can be found in Table S1. Similar extensions of terpenes oxidation are planned; the current study focuses on isoprene. In total 254 gas species are undergoing 779 chemical reactions including 146 photolysis, 16 stratospheric heterogeneous and 8 tropospheric heterogeneous reactions. The semi-explicit isoprene oxidation with 147 reactions constitutes a major of these reactions in JAM3.



Compound	SMILES code	$p_0^*(298.15\text{K})$ [Pa]	$\Delta H_{\text{vap}}$ [ $\frac{\text{kJ}}{\text{mol}}$ ]	$H$ [ $\frac{\text{mole}}{\text{atm}}$ ]
LNISOOH	<chem>O=CC(O)C(C)(OO)CON(=O)=O*</chem>	$2.2 \cdot 10^{-4}$	122.7	$2.1 \cdot 10^5$
	<chem>CC(O)(CON(=O)=O)C(OO)C=O</chem>	$3.8 \cdot 10^{-4}$	120.0	
LISOPOOHOOH	<chem>OC(C)(COO)C(CO)OO*</chem>	$3.8 \cdot 10^{-7}$	155.3	$2.0 \cdot 10^{16}$
	<chem>CC(CO)(C(COO)O)OO</chem>	$1.9 \cdot 10^{-7}$	158.9	
LC578OOH	<chem>OCC(O)C(C)(OO)C=O*</chem>	$2.0 \cdot 10^{-4}$	123.2	$3.0 \cdot 10^{11}$
	<chem>O=CC(O)C(C)(CO)OO</chem>	$2.0 \cdot 10^{-4}$	123.2	
C59OOH	<chem>OCC(=O)C(C)(CO)OO*</chem>	$1.0 \cdot 10^{-4}$	125.0	$3.0 \cdot 10^{11}$

**Table 1.** Isoprene oxidation products in JAM3, physical characteristics and molecular structure expressed as SMILES code. Saturation vapor pressure at the reference temperature 298 K  $p_0^*$ , Henry's law coefficient  $H$  and evaporation enthalpy  $\Delta H_{\text{vap}}$ .  $\Delta H_{\text{vap}}$  and  $p_0^*$  are used in Clausius Clapeyron equation for calculation of the saturation vapor pressure as a function of temperature in SALSA. Names of the compounds rely on the Master Chemical Mechanism (MCM 3.2), except for LISOPOOHOOH, which is not in MCM 3.2. Names starting with "L" indicate that this specie is lumped, SMILES codes of all isomers are shown, but just the ones marked with \* are used.

In order to identify SOA precursors produced via isoprene oxidation, first, for each specie a molecular structure was assigned. Some species are not represented explicitly, but instead they represent groups of compounds with similar chemical properties (lumping). In these cases a group of isomers were assigned to one structure. These structures are expressed as SMILES codes in Table 1 and as chemical structures in Figure 1. With those molecular structures, second, the saturation vapor pressure  $p^*(T)$  of each organic compound in JAM3 was estimated using the group contribution method by Nannoolal et al. (2008) and the boiling point method by Nannoolal et al. (2004) in the framework of the online open source facility UManSysProp (Topping et al., 2016). Third, the group contribution method data was fitted to the Clausius Clapeyron equation in order to determine the evaporation enthalpy  $\Delta H_{\text{vap}}$  for each compound. Finally, those species with saturation vapor pressures  $p_0^*$  at 298.15 K lower than 0.01 Pa were classified as low volatility compounds. This procedure leads to four low volatile isoprene oxidation products contributing to iSOA in ECHAM-HAMMOZ. Table 1 gives the SMILES codes and resulting saturation vapor pressure at the reference temperature  $p_0^*$  and the evaporation enthalpy  $\Delta H_{\text{vap}}$  for all low volatile iSOA precursors. The uncertainties in structure assignment of lumped species and the sensitivity to  $\Delta H_{\text{vap}}$  are explored in Sections 3.2.3 and 3.3.

Figure 1 shows the chemical pathways of isoprene oxidation and their products to form LIEPOX, LNISOOH, LISOPOOH-OOH, LC578OOH and C59OOH. For the whole chemical mechanism including IGLYOXAL formation, it is referred to the model description of HAMMOZ in Schultz et al. (submitted).

Low volatile isoprene oxidation products are formed in MOZ via several reaction steps. Four of these LVOCs were identified and their formation is based on two initial reaction pathways from the oxidation of isoprene by OH and  $\text{NO}_3$  respectively. Also the  $\text{O}_3$  initiated reactions pathways are included in MOZ, but none of the products was low volatile enough. The OH initiated pathway leads to three LVOCs called C59OOH, LC578OOH and LISOPOOHOOH in our mechanism. First, OH attacks isoprene  $\text{C}_5\text{H}_8$  and forms three isoprene peroxy radical isomers, where one of them is a lumped specie. For simplicity there are



called here ISOPO2.



ISOPO2 undergoes reactions with ambient radicals, but also self and cross reactions leading alcohols (ISOPHOH), isoprene hydroperoxides (ISOPOOH) and isoprene nitrates (ISOPNO3).



From the reactions of ISOPHOH and ISOPOOH with OH a hydroperoxide peroxy radical is formed, a lumped specie called LISOPOOHO2, which can be oxidized by HO<sub>2</sub> or CH<sub>3</sub>O<sub>2</sub> to LISOPOOHOOH. Not included is the H-shift of LISOPOOHO2 that yields much more volatile compounds than LISOPOOHOOH (Dambro et al., 2017b), so the chemical yield of LISOPOOHO-OOH is expected to be an upper estimate. LISOPOOHOOH has the highest yield of the LVOC considered here, 9% of

10 isoprene end up as LISOPOOHOOH.

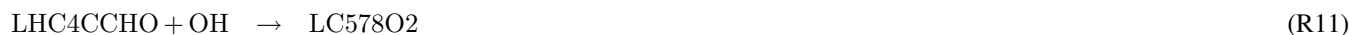
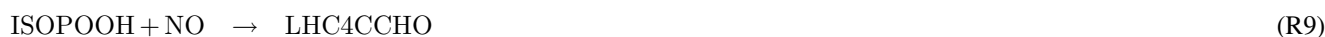


15 LISOPOOHOOH can either react back to LISOPOOHO2, be photolysed or oxidized by OH to form LC578OOH.



LC578OOH is another LVOC, which is more volatile than LISPOOHOOH and can be formed also via another pathway starting from ISOPO2, ISOPOOH and ISOPNO3, which either react with radicals, or in the case of the nitrate are photolysed leading to LHC4CCHO, which then reacts with OH to LC578O2. Finally, LC578O2 reacts with HO<sub>2</sub> and forms LC578OOH,

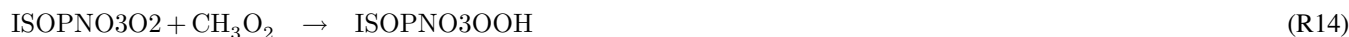
20 which either can react back to LC578O2 with OH or be photolysed. Just 1% of the oxidation of isoprene leads to LC578OOH.



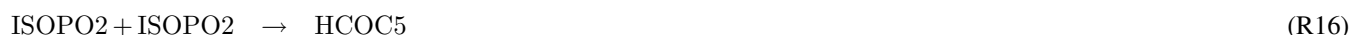
The third compound formed from the OH initiated oxidation of isoprene is C59OOH. Starting from ISOPO2, there are two possible oxidation ways for C59OOH formation, one with nitrates as intermediates and a second one where nitrogen oxide is not required. The nitrate pathway starts with formation of ISOPNO3 from ISOPO2 and continues with OH reaction to form



isoprene nitrate peroxy radicals ISOPNO3O2, which is again a lumped specie.



- 5 Via formation of a nitrate hydroxyperoxy radical, finally C59OOH is formed. This pathway requires the availability of NO. For the second pathway, no NO is needed.



- 10 Self-reactions of ISOPO2 lead to formation of HCOC5, which is then converted via OH to C59O2. HO2 oxidises C59O2 to C59OOH. C59OOH can also react back to C59O2 or be lost via photolysis. The overall yield from isoprene to C59OOH is 2%.

The fourth LVOC is an isoprene derived nitrate LNISOOH, which requires both, a NO<sub>x</sub> dominated and a HO<sub>2</sub> dominated environment, because only the first two oxidation steps use nitrate, then OH and HO<sub>2</sub> are required. First, isoprene reacts with

- 15 NO<sub>3</sub> radical and forms a nitrate peroxy radical NISOPO2, which oxidizes NO and forms NC4CHO. NC4CHO in contrast, has to react with OH to form LNISO3, which then reacts with HO<sub>2</sub> and forms LNISOOH.



- 20 LNISO3 → LNISOOH (R22)

LNISOOH can be photolysed or react back to LNISO3. Due to the requirements of both NO and HO<sub>2</sub> to be present, formation of LNISOOH is limited and this compound is only generated with a very low yield of just 0.1% from isoprene oxidation.

In Figure 1 the simplified overview over the described chemical reactions can be found. Reaction branching ratios from isoprene to the final compounds are shown as chemical structures used for the LVOCs. In the particle phase, the fraction which

25 ends up in the iSOA is expressed as percentage of total produced by partitioning LVOC and reactive uptake.

To cover multiphase chemical iSOA formation, heterogeneous reactions on aerosols of IEPOX and isoprene derived glyoxal were included. Nevertheless, ECHAM-HAMMOZ does not include in-particle or in-cloud aqueous phase chemistry, therefore no assumptions of in-particle products are made. Furthermore, no SOA formation via cloud droplets is included in ECHAM-HAMMOZ due to constraints in the aerosol cloud interaction formulation. Therefore, reactive uptake is parameterized as

30 pseudo first order loss using aerosol surface area density given by HAM, according to Schwartz (1986) and described in detail in Stadtler et al. (2017).

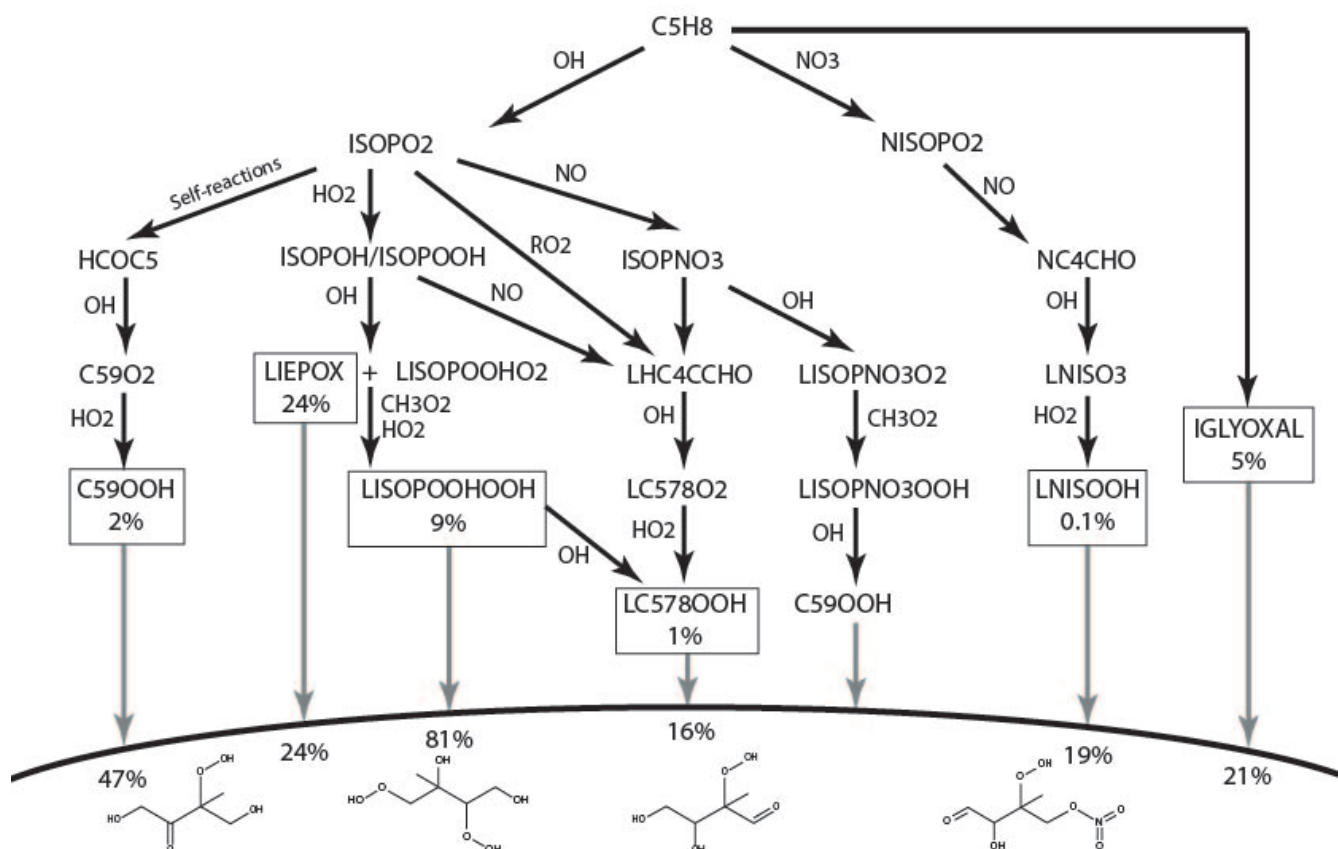


**Figure 1.** Simplified overview over chemical pathways leading to low volatile isoprene derived compounds able to partition into aerosol phase. Note that ISOPO<sub>2</sub> here is used for simplicity, JAM3 includes three different ISOPO<sub>2</sub> (LISOPACO<sub>2</sub>, ISOPBO<sub>2</sub>, ISOPDO<sub>2</sub>), same applies for ISOPOH and ISOPOOH. The percentages in the boxes indicate reaction turnover of isoprene leading to these products. For IGLYOXAL there are too many formation pathways and are therefore not shown. The solid horizontal curve represents the boundary to the particle phase. Percentages found under the corresponding arrow express the individual iSOA yield of the compound. Except for LIEPOX and IGLYOXAL, structures are relevant to estimate the saturation vapor pressure and evaporation enthalpy and are therefore shown here. For the detailed mechanism it is referred to Schultz et al. (submitted).



In MOZ, three IEPOX isomers are lumped together (LIEPOX) and a compound IGLYOXAL was introduced to be able to differentiate between isoprene derived glyoxal and glyoxal from other sources. Isoprene glyoxal formation pathways are numerous and no changes were made to the mechanism with respect to IGLYOXAL formation. Since these reactions are included also in JAM2, see Schultz et al. (submitted). LIEPOX is formed along the pathway described for LISPOOHOOH in Reaction, see (R3).

Glyoxal is observed to produce a variety of compounds, like oligomers or organosulfates, in the aqueous aerosol phase and glyoxal is capable of be released back in the gas phase (Volkamer et al., 2007; Ervens and Volkamer, 2010; Washenfelder et al., 2011; Li et al., 2013). The simplification assuming irreversible uptake might thus overestimate its impact on iSOA. Following previous model studies (Fu et al., 2008; Lin et al., 2012) a reaction probability of  $\gamma_{\text{glyoxal}} = 2.9 \cdot 10^{-3}$  (Liggio et al., 2005b) is used.

For IEPOX the irreversibility is a less critical assumption, because IEPOX forms 2-methyltetrol and organosulfates in the aqueous aerosol phase, which stay in the aerosol phase (Claeys et al., 2004; Eddingsaas et al., 2010; Lal et al., 2012; McNeill et al., 2012; Woo and McNeill, 2015). However, ECHAM-HAMMOZ does not include explicit treatment of aqueous phase reactions. The reaction probability of IEPOX varies with pH value (Lin et al., 2013a; Pye et al., 2013; Gaston et al., 2014) which cannot be captured by HAMMOZ due to the lack of ammonium and nitrate in the aerosol phase, thus the possibility to capture aerosol pH. For these reasons, the reaction probability of IEPOX  $\gamma_{\text{IEPOX}} = 1 \cdot 10^{-3}$  (Gaston et al., 2014) was chosen, close to the value used by (Pye et al., 2013). To explore the impact of the pH dependence sensitivity runs with different  $\gamma_{\text{IEPOX}}$  are analyzed. Additionally, no assumptions of in-particle products are made, in ECHAM-HAMMOZ IEPOX is simply taken up into aerosol phase without further transformation.

### 2.1.2 HAM-SALSA

The Hamburg Aerosol Model (HAM) handles the evolution of atmospheric particles and includes emissions, removal, microphysics and radiative effects. Moreover, the current configuration uses the Sectional Aerosol module for Large Scale Applications (SALSA) for calculation of aerosol microphysics (Kokkola et al., 2008). In SALSA the aerosol size distribution is divided into aerosol size sections (size bins). Furthermore, these size bins are grouped into sub-ranges, which allows the model to limit the computation of the aerosol microphysical processes to only the aerosol sized that are relevant to these processes. Microphysical processes simulated by SALSA cover nucleation, condensation, coagulation, cloud activation, sulfate production and hydration (Bergman et al., 2012). The aerosol composition is described using five different aerosol compounds, sulphate, black carbon, dust, sea salt and organic carbon. Furthermore, SALSA treats secondary organic aerosol formation via the volatility basis set (Kühn et al., in preparation). In the model setup described there, SALSA uses a strongly simplified description for VOC oxidation (pseudo chemistry) to obtain SOA precursors. Here this model system was extended and coupled to MOZ, which explicitly calculates SOA precursors as described in Section 2.1.1. The standard SALSA-VBS system is not used here. Instead for each SOA-forming compound the gas-to-particle partitioning is treated explicitly and its concentration is tracked in both the gas and the aerosol phases separately. This study exclusively uses isoprene-derived precursors to form iSOA, other oxygenated compounds capable of partitioning derived from terpenes or aromatics are neglected.



### 2.1.3 Coupling of HAM-SALSA and MOZ

HAM-SALSA and MOZ interact through several processes, oxidation fields calculated by MOZ are passed to HAM-SALSA for aerosol oxidation, MOZ produces  $\text{H}_2\text{SO}_4$  which is then converted by HAM-SALSA to sulphate aerosol and HAM-SALSA provides the aerosol surface area density for heterogeneous chemistry. Above all, HAM-SALSA takes the information of iSOA precursor gas phase concentrations and their physical properties to calculate the saturation concentration coefficient ( $C^*$ ) using Clausius Clapeyron equation (1) (Farina et al., 2010).

$$C_i^* = C_i^*(T_0) \frac{T_0}{T} \exp \left[ \frac{\Delta H_{vap}}{R} \left( \frac{1}{T_0} - \frac{1}{T} \right) \right] \quad (1)$$

Here  $T_0$  is the reference temperature of 298.15 K and  $\Delta H_{vap}$  is the evaporation enthalpy given in Table 1 for the iSOA precursors identified in this study.  $C^*$  is then used to calculate the explicit partitioning of the iSOA precursors to each aerosol section. This process is reversible and it is thus possible that the iSOA formed in one region is transported and evaporates in another region. Explicitly calculating the partitioning instead of prescribing yields in chemical production or SOA formation is a key difference to other models with fixed yields. Loss processes for SOA in HAM-SALSA include sedimentation, deposition and wash out in the aerosol phase.

## 2.2 Simulation set up and sensitivity runs

An overview of the performed simulations can be found in Table 2. The reference simulation RefBase, which includes a three-month spin up and spans the time from October 2011 until the end of December 2012, is evaluated for the entire year 2012, while all other sensitivity runs are limited to the northern hemispheric, isoprene emission intense, summer season of June, July and August.

Several sensitivity simulations were performed to explore model sensitivities and assess uncertainties. For comparison of the explicit ECHAM-HAMMOZ scheme to a state-of-the-art VBS scheme, ECHAM-HAM with pseudo chemistry and VBS configuration (RefVBS), described in 2.1.2, was run.  $\Delta H_{30}$  uses the same, much lower evaporation enthalpy of  $\Delta H_{vap} = 30 \frac{\text{kJ}}{\text{mol}}$  for all partitioning LVOC following Farina et al. (2010). Furthermore, pH value dependence of IEPOX is tested in  $\gamma$ IEX formulating an easy pH dependent parameterization based on laboratory measurements. Particle pH values cannot be obtained from ECHAM-HAMMOZ itself as the model does not include the calculation of particle phase thermodynamics. For this reason, aerosol pH was calculated offline using the AIM aerosol thermodynamics model (Clegg et al., 1998). The SALSA simulated annual mean mass of aerosol water and the mean mass of aerosol-phase inorganic compounds at the lowest model level were used as an input for AIM. This required two additional assumptions: (1) all aerosol is in liquid form, (2) all sulfate is in form of ammonium bisulfate. This second assumption for sulfate has to be done, because particle phase ammonia is not modeled in the current configuration of ECHAM-HAMMOZ. Using these inputs, AIM provided the concentration of hydrogen ion ( $\text{H}^+$ ) as an output.



Simulation	Description
RefBase	Reference run with uniform reaction probabilities for IEPOX and isoprene glyoxal $\gamma_{IEPOX} = 1.0 \cdot 10^{-3}$ , $\gamma_{IGYOXAL} = 2.9 \cdot 10^{-3}$ (see Section 2.1.1), LVOC $\Delta H_{vap}$ and $p_0^*$ (298.15K) given in Table 1.
RefVBS	VBS approach with pseudo chemistry.
$\Delta H30$	Run like reference run, but with same $\Delta H_{vap} = 30 \frac{kJ}{mol}$ for all compounds.
$\gamma pH$	Like RefBase, but with $\gamma_{IEPOX} = f(pH)$ .

**Table 2.** Description of simulations performed.

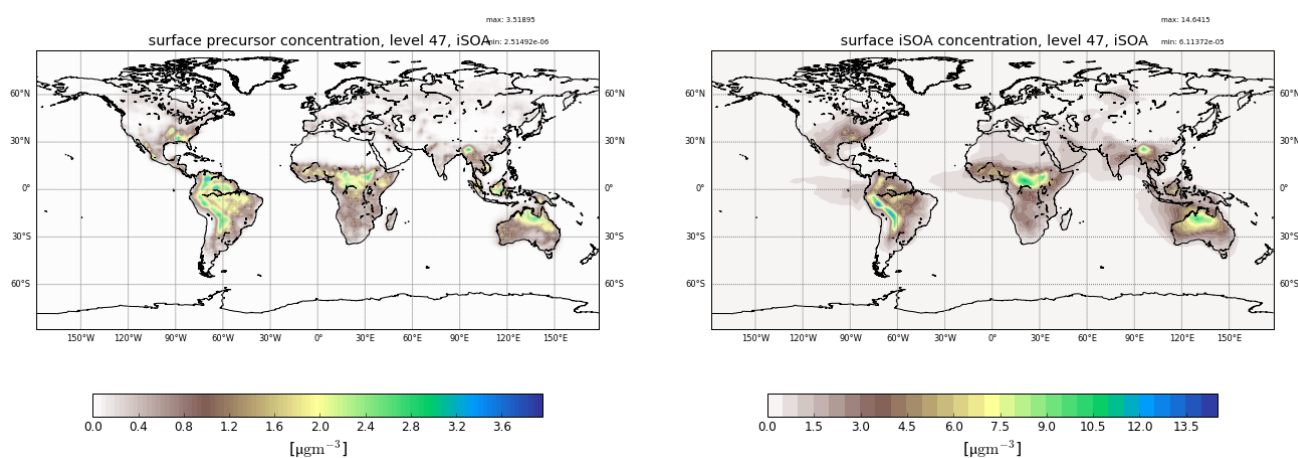


**Figure 2.** Reference run annual average surface distribution of precursor gases and iSOA in  $\mu\text{g m}^{-3}$  for 2012.

### 3 Results

#### 3.1 Reference run RefBase

##### 3.1.1 Global distributions

Figure 2 shows the annual mean surface concentrations for total iSOA and its precursors in the gas phase. The precursors are formed, except for LNISOOH, during daytime and build up quickly. Therefore, these are found very close to isoprene source regions mostly in the tropics and southern hemisphere. Their highest values, up to  $3 \mu\text{g m}^{-3}$ , are simulated over the Amazon, the east flank of the Andes, Central Africa, North Australia, Indonesia and Southeast Asia. In the annual mean also the northern hemispheric summer is visible, but peak values of over  $2 \mu\text{g m}^{-3}$  are only reached on Mexico's west coast and in the southeastern US. In Europe and North Asia, where isoprene emissions are much lower, mean values up to  $0.5 \mu\text{g m}^{-3}$  of precursors are formed.



These low precursor concentrations correspond to the very low iSOA concentrations over Europe and North Asia, compared to Southeastern US and Mexico's west coast, where up to  $4.5 \mu\text{g m}^{-3}$  iSOA is formed. The highest iSOA concentrations are found where high precursor concentrations meet pre-existing aerosol, like in Central Africa because of its high biomass burning emissions or Southeast Asia, where aerosol pollution is high. In the latter ECHAM-HAMMOZ simulates values of up to  $13 \mu\text{g m}^{-3}$  if iSOA. The Amazon is a region of very high isoprene emissions and therefore high iSOA precursor concentrations, nevertheless the local maximum in iSOA of  $14 \mu\text{g m}^{-3}$  can be seen on the east side of the Andes. This pattern is caused by pre-existing aerosol, which in ECHAM-HAMMOZ tends to accumulate on the east side of the Andes, and the still high iSOA precursor concentrations in the same region. Also in the northern part of Australia higher precursor loadings are found, leading there to iSOA ground-level concentrations of up to  $9 \mu\text{g m}^{-3}$ .

It can also be seen, that iSOA has a longer lifetime than its gas-phase precursors. Prevailing wind directions are recognizable, clearly showing transport of iSOA over the oceans, for example in the South American and African outflow regions. Also, iSOA is transported from Australia to the north. The average iSOA lifetime was calculated to be around 4 days, so long-range transport is limited, before iSOA is lost due to wet deposition (see Section 3.1.2).

Farina et al. (2010) included iSOA formation with fixed yields of isoprene transformation to the different VBS classes and also showed its global annual surface distribution for 1979 - 1980. Compared to Farina et al. (2010) ECHAM-HAMMOZ simulates nearly one order of magnitude higher maximum iSOA concentrations. This is explained by much higher reaction turnover from MOZ leading to higher amounts of iSOA precursors than produced by the low yields prescribed in Farina et al. (2010). The global patterns agree in high values over Southeastern US, South America, Central Africa and North Australia. In contrast, Farina et al. (2010) do not simulate the maximum over Southeast Asia. Hodzic et al. (2016) show biogenic SOA for the lower 5 km on a global scale, again general patterns agree with the distribution in ECHAM-HAMMOZ. Nevertheless, Hodzic et al. (2016) simulated higher concentrations over Eurasia, which is not captured by ECHAM-HAMMOZ due to the lack in other BVOC derived SOA. Total biogenic SOA concentrations with iSOA surface concentrations of ECHAM-HAMMOZ compare well with their order of magnitude, which again underlines the higher yields resulting in ECHAM-HAMMOZ. High concentrations result from the highly oxidized compounds produced by MOZ chemistry, especially LISPOOHOOH molar mass of  $168.14 \text{ g mol}^{-1}$  is very large. LISPOOHOOH and LIEPOX contribute most to iSOA, followed by isoprene glyoxal. To further discuss this, iSOA composition concentrations for northern hemispheric summer (June, July, August) are shown in Figure 3.

Figure 3 shows on the left hand side gas phase precursor concentrations. First, LIEPOX and LISPOOHOOH are shown, because they have greatest impact in the particle phase, followed by IGLYOXAL. The other iSOA precursor LVOCs are shown together because of their low concentrations in gas and particle phase. On the right hand side corresponding mean values in the particle phase are displayed.

From the gas phase LIEPOX distribution it can be seen that MOZ simulates concentrations of around  $0.5 \mu\text{g m}^{-3}$  over isoprene rich areas. Peak values of  $4.5 \mu\text{g m}^{-3}$  LIEPOX are found over Southeastern US, north Venezuela and North of Myanmar. Higher concentrations of LIEPOX are reached in the aerosol phase for example in South America gas phase concentrations varies between  $1.5$  and  $2.5 \mu\text{g m}^{-3}$ , but LIEPOX-SOA values over  $7 \mu\text{g m}^{-3}$  are reached on the eastern edge

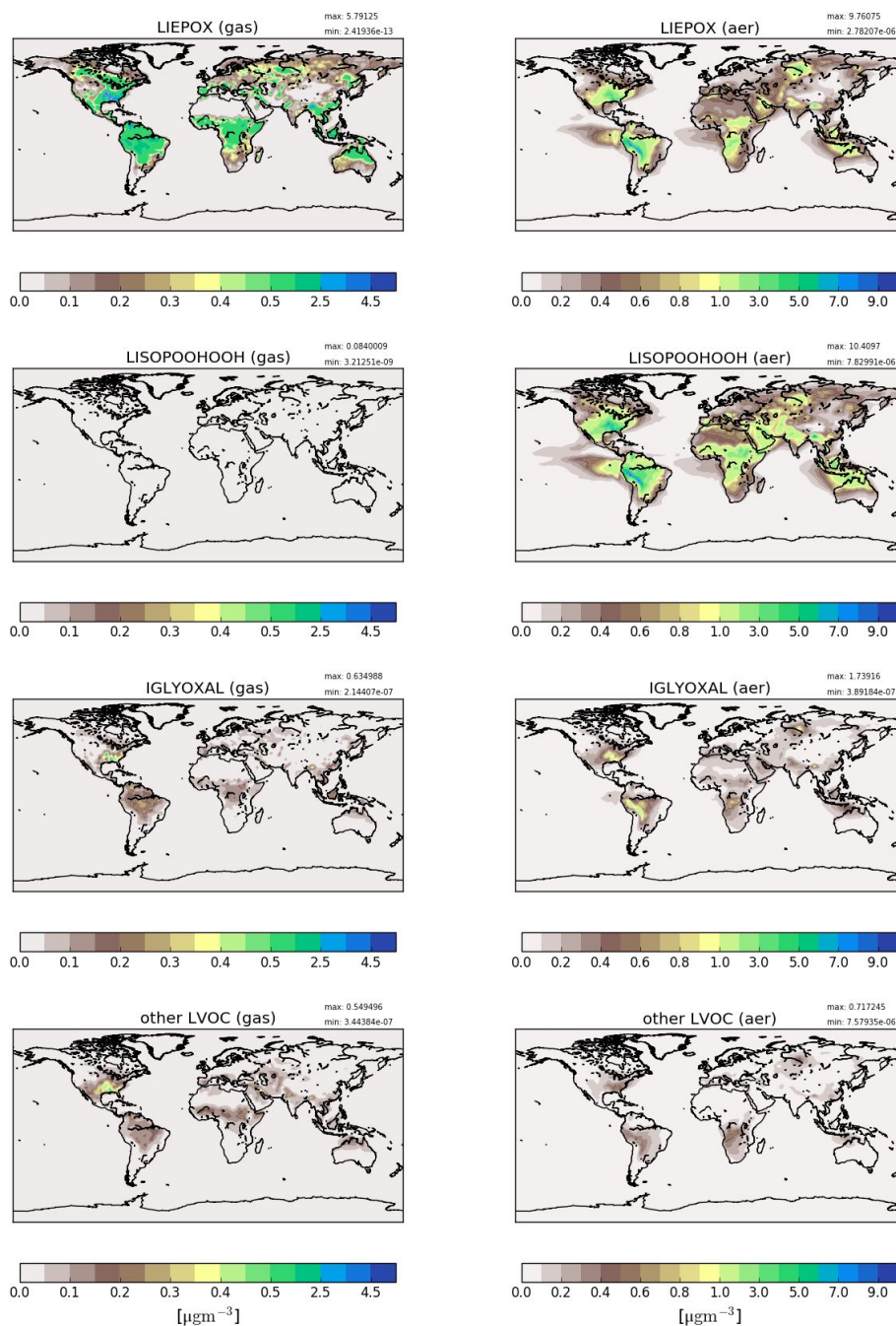


**Figure 3.** Reference run average surface distribution of precursor gases (left) and corresponding component concentration in the particle phase (right) in  $\mu\text{g m}^{-3}$  for June, July and August 2012. Since concentrations of non LISPOOOHOOH LVOC are quite low, they are shown together. Different scales are used for precursors and iSOA to capture the concentration ranges accordingly. Note, that the concentration scales are not linear and focus on low concentrations.



of the Andes. Especially LIEPOX-SOA transport over the ocean and over Sahara can be seen. No assumption of in-particle products for LIEPOX was made, but usually 2-methyltetrols in the order of  $\text{ng m}^{-3}$  are measured in the particle phase (Claeys et al., 2004; Kourtchev et al., 2005; Clements and Seinfeld, 2007). Lopez-Hilfiker et al. (2016) report that 80% of IEPOX forms dimers instead of 2-methyltetrols, which would increase the concentrations of IEPOX derived SOA in the ambient measurements. Accounting additionally for these 80%, the mass concentrations would reach around  $10\text{-}100 \text{ ng m}^{-3}$ , still an overestimation of simulated LIEPOX-SOA is indicated.

In contrast to LIEPOX, LISOPOOHOOH gas phase concentrations are very low and even with a scale focusing on low values, these cannot be captured on a scale fitting to the other compounds. For the gas phase LISOPOOHOOH globally lower values than  $0.1 \mu\text{g m}^{-3}$  are calculated. This is a consequence of iSOA formation. On the LISOPOOHOOH-SOA plot can be seen, that it appears in quite big amounts in the particle phase, because it is extremely low volatile. Depending on the region, even more iSOA is formed by LISOPOOHOOH than LIEPOX, like over the Middle East. Indeed, the sum of LIEPOX and LISOPOOHOOH make up to 90% of iSOA mass.

IGLOYXAL and the sum of the other LVOC show similar global distributions and concentrations. Nevertheless, reactive uptake is more efficient producing more IGLOYXAL-SOA than from the other LVOC. IGLYOXAL shows similar maxima as LIEPOX over the American continent, North of Myanmar and over Siberia. Whereas the sum of other LVOC shares areas of peak values with LISOPOOHOOH, pointing out the different iSOA formation processes. Similarly, up to 8% of iSOA is formed by IGLOYXAL, the rest of 2% mainly consist of C59OOH

Particle concentrations seem quite high taking into account, that possible isoprene IVOC and SVOC were excluded. Hodzic et al. (2016) claimed, that SOA production might be stronger, but also removal processes, which are currently ignored by global models. These removal processes include fragmentation, aqueous phase reactions, in-particle photolysis. As seen in Section 3.1.2, iSOA production in ECHAM-HAMMOZ is quite high, leading to these concentrations. Including more aerosol sinks following Hodzic et al. (2016) could reduce these concentrations even if iSOA production remains high.

To summarize, Figure 3 shows that particle formation does not only depend on precursor concentrations, but also on available preexisting aerosol. Since all compounds are produced by isoprene the global distribution of the individual gases does not differ a lot. In contrast to the annual mean, the Northern Australian maximum does not appear that prominently here. Hence, the great impact in Northeastern US is clearly visible. For Europe, even during summer, iSOA seems to play a minor role compared to the equatorial regions due to prevalent vegetation (Steinbrecher et al., 2009).

### 3.1.2 Global iSOA budget

The global annual budget for isoprene derived secondary organic aerosol is shown in Figure 4. For the evaluated simulation period of 2012 a total of 391.6 TgC isoprene were emitted, which is a bit lower than the range of estimated isoprene emissions 440 - 660 TgC (Guenther et al., 2006; Henrot et al., 2017). The oxidation of isoprene leads to production of 160.8 TgC of the six iSOA precursors identified in this study. Comparing it to the initially emitted amount, 41% of isoprene is chemically transformed into iSOA precursors. 24% of isoprene end up in IEPOX, 9% in LISOPOOHOOH, 5% in IGLYOXAL, 2% in C59OOH, 1% in LC578OOH and 0.1% in LNISOOH (see Table 3). For LIEPOX 93.5 TgC are produced, which agrees very



Specie	Gas phase production in TgC (fraction of isoprene source)	Particle formation in TgC (individual yield in %)
LIEPOX	93.5 (24%)	24.4 (24%)
IGLYOXAL	19.8 (5%)	4.1 (21%)
LISOPHOHOH	34.9 (9%)	28.3 (81%)
C59OOH	7.1 (2%)	3.3 (47%)
LC578OOH	4.9 (1%)	0.8 (16%)
LNISOH	0.5 (0.1%)	0.1 (19%)

**Table 3.** Total annual chemical production of individual iSOA precursors 2012 and corresponding amount of iSOA formed. In parenthesis the corresponding yields are given, for the gas phase how much of total isoprene was converted to the precursors and the yield of those precursors into iSOA for the global annual budget.

well with  $95 \pm 45$  TgC estimated by Paulot et al. (2009). Of the total produced iSOA precursors, about a third (61.0 TgC) form iSOA. Half of iSOA is formed by reactive uptake, where IEPOX contributes 24.4 TgC and glyoxal 4.1 TgC, corresponding to a reactive uptake yield of 25% (LIEPOX) and 23% (IGLYOXAL), respectively. Since the reactive uptake is irreversible and the partitioning species can be classified as very low volatile compounds, evaporation is several orders of magnitude lower than condensation. This results in an annual overall isoprene SOA yield of 16 %, and in a global burden of 0.7 TgC. A isoprene SOA yield of 16% lies in the range of 1% to 30% under different conditions observed by Surratt et al. (2010). Sinks of the precursor gases are chemical loss including photolysis, dry and wet deposition. The main part of precursors is destroyed chemically, the second most important sink is wet deposition. Aerosols can be lost via three processes in ECHAM-HAMMOZ, via sedimentation, dry and wet deposition. For iSOA sedimentation is less than 0.5 TgC and is for a clearer structure not included in Figure 4. The main loss of iSOA is wet deposition removing 59.1 TgC of the total of 61.0 TgC.

Table 4 shows the iSOA budget in Tg to be comparable with the mean values of the AeroCom (Aerosol Comparisons between Observations and Models) given in Tsigaridis et al. (2014). As can be seen from Table 4, the iSOA production of ECHAM-HAMMOZ in the reference simulation exceeds total SOA of the AeroCom models in the upper third quartile limit. Even if this comparison here seems to show a vast overestimation by ECHAM-HAMMOZ 61 TgC iSOA do not reach the lower end of the top down estimated source strength ranging from 140 - 910 TgC a<sup>-1</sup> (Goldstein and Galbally, 2007; Hallquist et al., 2009). Therefore, according to these studies, the AeroCom models generally produce too little SOA, while our new approach might lead to more realistic SOA concentrations. Using the range of 140 - 910 TgC a<sup>-1</sup> for total SOA and our iSOA production of 61 TgC a<sup>-1</sup> would imply that isoprene contributes between 7% and 43% to total SOA. This does not seem unrealistic. Dry deposition and wet deposition are higher than the AeroCom mean value, because iSOA burden is larger. Nevertheless, in ECHAM-HAMMOZ wet deposition is more than ten times higher than dry deposition, something that is not seen in the AeroCom models. First, this might point to a too low aerosol dry deposition in ECHAM-HAMMOZ. Second, high wet deposition might be caused by moisture and convection overestimation of ECHAM6 in the tropical regions where most of iSOA is formed. Finally, the iSOA burden in ECHAM-HAMMOZ is also higher than the mean of AeroCom models, while iSOA life time of 4.2 days is in the lower end, which can also be explained by the huge wet deposition loss.

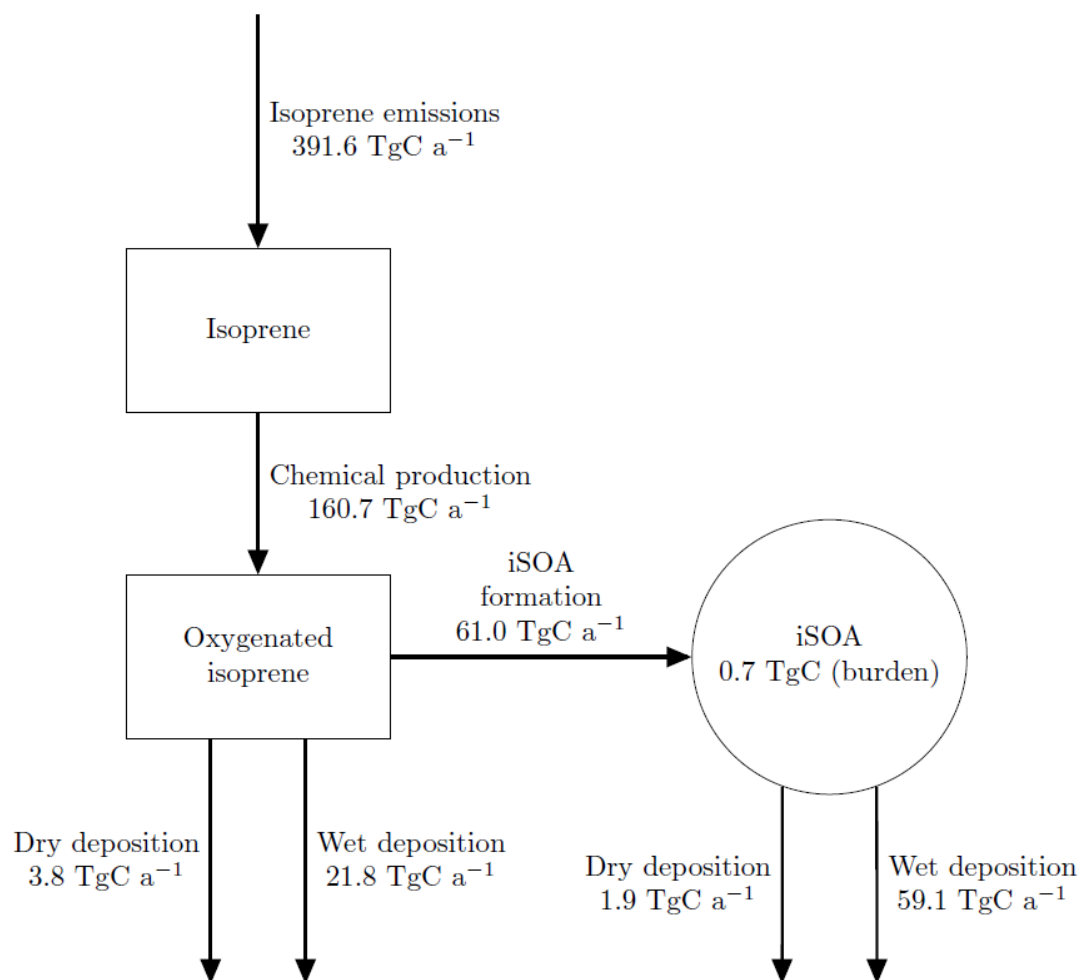


**Figure 4.** Global budgets for isoprene derived secondary organic aerosol and its precursors (sources/sinks in  $\text{TgC a}^{-1}$  and burden in  $\text{TgC}$ ) predicted by ECHAM-HAMMOZ reference simulation for 2012. For details about the individual compounds see Table 3.

	ECHAM-HAMMOZ	AeroCom mean	AeroCom range
Sources	147.8 $\text{Tg a}^{-1}$	36.3 $\text{Tg a}^{-1}$	12.7 - 120.8 $\text{Tg a}^{-1}$
Dry deposition	4.7 $\text{Tg a}^{-1}$	5.7 $\text{Tg a}^{-1}$	1.4 - 14.5 $\text{Tg a}^{-1}$
Wet deposition	143.1 $\text{Tg a}^{-1}$	47.9 $\text{Tg a}^{-1}$	12.4 - 113.1 $\text{Tg a}^{-1}$
Burden	1.6 Tg	1.0 Tg	0.3 - 2.3 Tg
Lifetime	4.2 days	8.2 days	2.4 - 14.8 days

**Table 4.** Comparison of the ECHAM-HAMMOZ iSOA budget to total SOA budget terms from AeroCom models mean value in OA budgets (Tsigaridis et al. (2014), personal communication).



As stated in Hodzic et al. (2016), global models are missing aerosol sinks like in particle fragmentation and particle photolysis and should therefore overestimate SOA formation. On the contrary, global models tend to underestimate SOA formation. The comparison of ECHAM-HAMMOZ iSOA is to total SOA of other models shows that the criticized underestimation is more than resolved, since no SOA from aromatics or terpenes is considered in this study. Including semi-explicit chemistry and explicit partitioning leads in ECHAM-HAMMOZ to a high isoprene SOA yield, which motivated several sensitivity runs.

## 3.2 Sensitivity runs

### 3.2.1 Comparison to pseudo chemistry SOA

As explained in Section 2.1.2 ECHAM-HAM with SALSA has an own module to simulate SOA formation via the VBS system using pseudo chemistry to form SOA precursors. To compare the semi-explicit chemistry and explicit compound-wise partitioning to the pseudo chemistry and VBS system, an ECHAM-HAM run (RefVBS) was performed just including isoprene emissions to form just iSOA in both models. From these isoprene emissions ECHAM-HAM produces gas phase compounds of the VBS classes 0, 1 and 10. Therefore, also semi volatile compounds are included, which lack in RefBase. Conversely, ECHAM-HAM does not include IEPOX and glyoxal SOA, thus here these two compounds are not included in the comparison. Total iSOA formed by partitioning including SVOC and IVOC from ECHAM-HAM RefVBS is compared to iSOA from LVOC in ECHAM-HAMMOZ reference run RefBase.

The formed precursors in the gas phase from RefVBS compared to the LVOC from RefBase are shown in Figure 5. From the higher gas phase concentrations, it can be seen that the VBS system also includes semi volatile compounds. Again, the emission pattern of MEGAN is clearly visible on both model runs, just very low concentrations in RefBase hide some isoprene emitting areas.

Nevertheless, the low gas phase concentrations in RefBase do not mean, that less iSOA precursors were formed, in contrary as can be seen in Figure 5 iSOA from LVOC in RefBase is overall higher and horizontally transported further than iSOA in RefVBS. Local maxima match between both models, the higher values in Southeastern US and in the Amazon are captured by both models. However, in Southeastern US RefBase simulates values around  $6 \mu\text{g m}^{-3}$  over a broader area than RefVBS reaching  $3.5 \mu\text{g m}^{-3}$  in two more local maxima. Similarly, over the Amazon and north of the Andes RefBase simulates up to  $9 \mu\text{g m}^{-3}$  while RefVBS reaches  $3 \mu\text{g m}^{-3}$ . Both simulations also agree on a local maximum in Central Africa and over North Australia and Indonesia. Again, peak concentrations differ, here by a factor of around 2.

Even if RefVBS includes also SVOC in their iSOA formation, particle concentrations are higher in RefBase. This results from different chemical precursor formation, via semi-explicit MOZ LVOC are formed in an amount large enough to make significant contributions to SOA mass. LISOPHOHOH formations is not taken into account in the ECHAM-HAM pseudo chemistry formulation and explain comparably low iSOA yields accounted for.

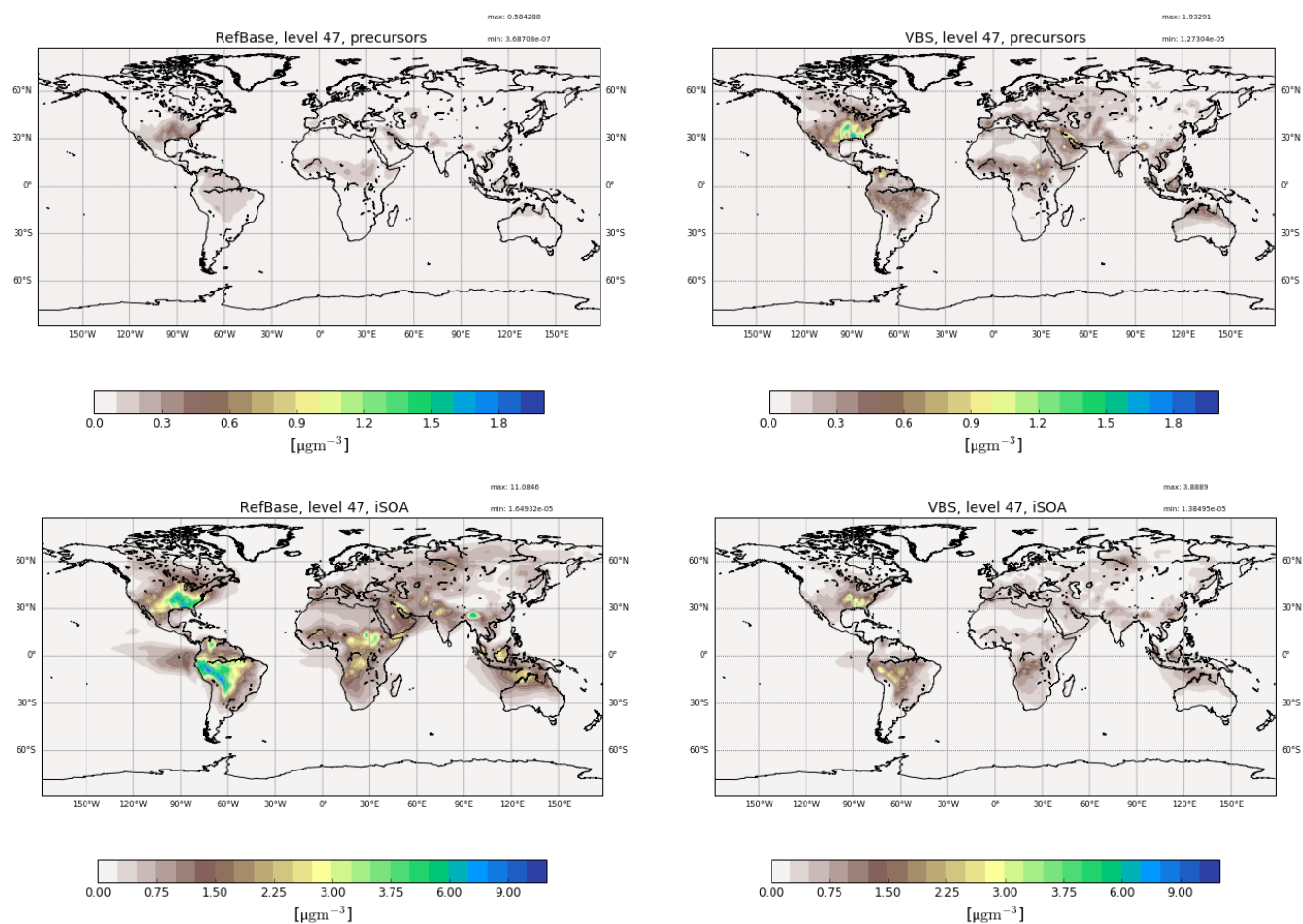


**Figure 5.** Seasonal mean values of gas phase precursors (upper plots) and iSOA (lower plots) for June, July and August 2012 at the surface layer. The reference run RefBase with ECHAM-HAMMOZ is shown on the left side, on the right the ECHAM-HAM RefVBS. For RefBase the precursors consist of the four isoprene derived LVOC described above, for RefVBS the sum of gas phase VBS classes 0, 1 and 10 is shown.

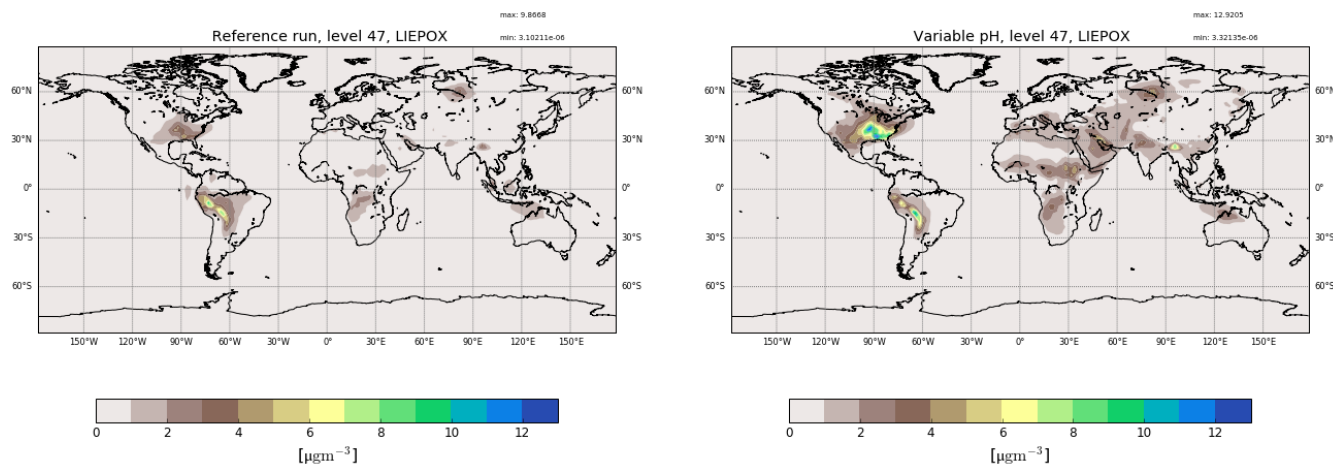


**Figure 6.** Surface aerosol concentrations for LIEPOX derived iSOA with uniform pH value used in the reference run (left) and with variable pH value calculated with AIM aerosol thermodynamics model (see Section 2.2) in the sensitivity run  $\gamma$ pH for the time period of June, July and August 2012.

### 3.2.2 IEPOX sensitivity to aerosol pH

As discussed in Section 2.1.1, several laboratory and field studies suggested a pH value influence on the reactive uptake of IEPOX. ECHAM-HAMMOZ does not include ammonium and nitrate aerosol, therefore no aerosol pH value can be obtained by the model system. As described in Section 2.2 a simulation with AIM aerosol thermodynamics model was performed to obtain the global aerosol pH distribution consistent to ECHAM-HAMMOZ aerosols (Figure S1). Aerosol pH distribution by AIM is used as input in the sensitivity simulation  $\gamma$ pH, while the reference simulation RefBase uses a uniform value for the reactive uptake coefficient  $\gamma$  corresponding to a pH of around 2.5. The simulation  $\gamma$ pH was designed to explore the impact of such a dependence. Therefore, based on reaction probability values given in Eddingsaas et al. (2010) and Gaston et al. (2014) a simple function for  $\gamma_{IEPOX}$  was formulated and implemented in ECHAM-HAMMOZ:

$$\gamma(\text{pH}) = \begin{cases} 10^{-2}, & \text{pH} < 2 \\ 0.1[\text{H}^+] + 10^{-4}, & \text{pH} \in [2, 5] \\ 0, & \text{pH} > 5 \end{cases} \quad (2)$$

where  $[\text{H}^+]$  is the concentration of protons  $\text{H}^+$  in the aerosol given in  $\text{mol l}^{-1}$ . The reaction probability varies linearly between particles of pH values between 2 and 5. For acidic particles the upper limit of  $10^{-2}$  is fixed. For particles which are not acidic enough (pH greater 5) no reaction is assumed. The pH distribution (Figure S1) was then used as model input values. The pH value of the surface aerosols was applied to each model layer, but largest effect can be observed where acidic aerosol and LIEPOX are present.



Figure 6 shows the resulting global surface distribution of  $\gamma$ pH run for northern hemispheric summer compared to RefBase. Enhancement of reactive uptake in  $\gamma$ pH over land is clearly visible, especially over Southeastern US maximum values are more than doubled. Further, more areas with 3 - 4  $\mu\text{g m}^{-3}$  over Africa, the Middle East and Eurasia can be found, where RefBASE has values lower than 1  $\mu\text{g m}^{-3}$ . In contrast, suppression of LIEPOX reactive uptake is observable over the Amazon.

5 Total LIEPOX aerosol produced during this time period increased by 58% in  $\gamma$ pH compared to RefBase. In RefBase an aerosol pH around 2.5 was assumed for all aerosols, also those which might be less acidic like sea salt aerosol. Nevertheless, compared to  $\gamma$ pH less LIEPOX-SOA was formed. In  $\gamma$ pH most areas are covered by less acidic aerosol but LIEPOX is produced or transported there, where acidic aerosol can be found, this leads to the observed increase in iSOA formation.

As an alternative explanation for the to pH value dependence, Xu et al. (2015) hypothesize that LIEPOX uptake enhancement  
10 could be triggered by sulfate aerosol. Although sulfate aerosol is simulated no sensitivity study was performed here due to lack of process understanding and possible reactive uptake parametrizations.

### 3.2.3 Sensitivity to evaporation enthalpy

Tsigradis and Kanakidou (2003) point out the sensitivity of SOA formation to the evaporation enthalpy  $\Delta H_{vap}$ . Nevertheless, due to the lack of knowledge of  $\Delta H_{vap}$  of the various different organic compounds, usually a fixed value or rather low value is  
15 used for all of them (Epstein et al., 2009). Depending on the study, different estimations for  $\Delta H_{vap}$  were made, ranging between 30 and 156  $\text{kJ mol}^{-1}$  (Athanasopoulou et al., 2012). Farina et al. (2010) also use the Clausius-Clapeyron equation to calculate saturation concentrations for a variety of organics using for all of them 30  $\text{kJ mol}^{-1}$ . To explore the impact of this assumption and the impact of a lower evaporation enthalpy, the sensitivity run  $\Delta H30$  was designed to use  $\Delta H_{vap} = 30 \text{ kJ mol}^{-1}$  but keeping the same reference saturation vapor pressure (see Table 1).

20 As an example Figure 7 shows the curves given by equation (1) using  $\Delta H_{vap}$  of the reference run and the sensitivity run. Equation (1) changes its curve form drastically when lowering  $\Delta H_{vap}$  from values around 150  $\text{kJ mol}^{-1}$  to 30  $\text{kJ mol}^{-1}$ . For temperatures lower than the reference value of 298.15 K the saturation vapor pressure of  $\Delta H30$   $p_{\Delta H30}^*$  is higher compared to the reference  $p^*$ , but for temperatures higher 298.15 K the opposite is the case (see Figure 7).

As a result, the impact of variable  $\Delta H_{vap}$  on iSOA formation varies with temperature, therefore, also with region and  
25 height. The sensitivity simulation  $\Delta H30$  ran for June, July and August 2012 with changed Clausius-Clapeyron equation curves according to Figure 7. Even during this northern hemispheric summer, on a global perspective the atmosphere is on average cooler than 298.15 K, especially at higher altitudes. Therefore, global total iSOA production in  $\Delta H30$  for the considered time period is just 0.6 TgC lower compared to RefBase. This is a reduction of 4% of the total amount produced in RefBase in June, July and August 2012. For surface temperatures higher than 298.15 K  $p_{\Delta H30}^*$  is orders of magnitude lower than the reference  
30  $p^*$ , but gas phase concentrations of iSOA precursors are high enough, that no significant impact on iSOA concentrations is seen. In agreement, surface concentration fields do not change much and are therefore not shown.

The assumption made by Farina et al. (2010) connected with the estimation of LVOC  $p_0^*$  in this study therefore does not lead to significant changes in model results. Lowest sensitivity to  $\Delta H_{vap}$  can be found in the lowest LVOC, LISOPHOHOH. In

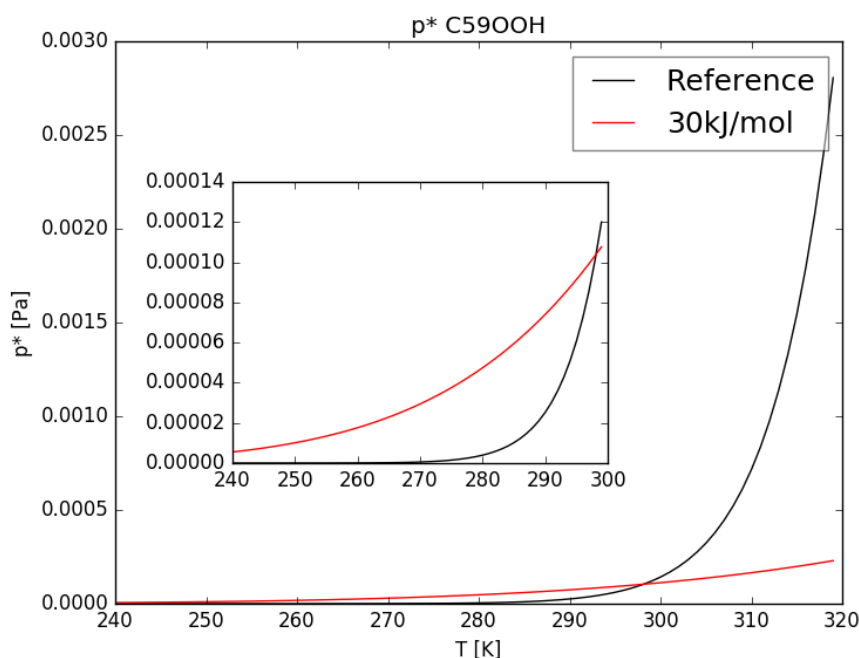


**Figure 7.** Curves given by Clausius Clapeyron equation 1 for C59OOH. The red curve is obtained by setting  $\Delta H_{vap} = 30 \text{ kJ mol}^{-1}$ , the black one describes the parameters used in the reference run (see Table 1).

ECHAM-HAMMOZ sensitivity to  $\Delta H_{vap}$  increases with volatility of the compounds, therefore  $\Delta H_{vap}$  should be crucial for additional consideration of SVOC and IVOC, which will be added to the model in a future study.

### 3.3 Uncertainty estimation saturation vapor pressure

As described in Section 2.1.1 the group contribution method by Nannoolal et al. (2008) in combination with the boiling point method by Nannoolal et al. (2004) were used to obtain the saturation vapor pressure of originated isoprene products as a function of temperature. Group contribution methods estimate the contribution of functional groups on saturation vapor pressure. The Nannoolal et al. (2008) group contribution method is based on 68835 data points of 1663 components and just needs two inputs, the molecular structure and the normal boiling point. Nannoolal et al. (2008) report a good performance against measurements. Nevertheless, when its performance is compared to compounds outside the training set, results become worse (Barley and McFiggans, 2010; O'Meara et al., 2014). Barley and McFiggans (2010) underline that databases are typically biased towards mono-functional groups and therefore, group contribution methods trained with these data perform well at volatile fluids, but not for low volatility compounds. O'Meara et al. (2014) arrive at similar conclusions, they tested seven saturation vapor pressure estimation methods and found that even if Nannoolal et al. (2008) method results in the lowest mean bias error, the method shows poor accuracy for compounds with low volatility. This tendency holds also true for the other



	Nannoolal et al. (2008)	Donahue et al. (2011)
LNISOOH	1.2 (1.4)	1.3
LISOPOOHOOH	-1.6 (-1.9)	-0.7
LC578OOH	1.1 (1.1)	1.
C59OOH	0.8	1.

**Table 5.** Comparison logarithmic saturation concentrations  $\log_{10}C_0^*$  at 300 K for the LVOCs calculated via the group contribution method used here (Nannoolal et al., 2008) and a simple group contribution method formulated by Donahue et al. (2011). In brackets the  $\log_{10}C_0^*$  for the isomers are shown.

tested methods showing an increasing error with increasing number of hydrogen bonds. This systematic error results in a SOA formation overestimation. Moreover, McFiggans et al. (2010) analyzed the dependence of SOA formation of the saturation vapor pressure of each compounds and state that SOA mass is highly sensitive to this parameter. Up to 30% overestimation can result from ignoring non-ideality of the organic mixture.

5 These studies already identified and emphasized several causes and consequences of the various group contribution methods. Thus,  $\log_{10}C_0^*$  values are compared to a simple group method based on oxygen, carbon and nitrate atoms in the molecule described in Donahue et al. (2011) (Table 5).

As can be seen from Table 5, the  $\log_{10}C_0^*$  values do not differ much between the simple group contribution method of Donahue et al. (2011) and the one by Nannoolal et al. (2008), except for the lowest volatility compound LISOPOOHOOH. 10 For LISOPOOHOOH, Nannoolal et al. (2008) predict a much lower volatility than Donahue et al. (2011). This difference agrees with the findings of the studies described above and indicates that LISOPOOHOOH-iSOA formation might be too high in ECHAM-HAMMOZ. Also given are the  $\log_{10}C_0^*$  values for the different isomers. Due to computational resource limits, no further sensitivity runs were done. Nevertheless, from the  $\log_{10}C_0^*$  values and the values in Table 1 it is clear, that for LC578OOH there is no difference caused by isomeric structures in volatility, for LNSISOOH the other isomer is even slightly 15 more volatile and for LISOPOOHOOH the opposite holds true, its second isomer is slightly less volatile. Since LNISOOH is only formed in very low concentrations these deviations might not be visible in iSOA formation. Similarly an even lower volatility LISOPOOHOOH should also not change the main findings of this study, since it already dominates iSOA formation.

### 3.3.1 Comparison with observations

In order to evaluate how much of total organic aerosol (OA), including primary and secondary organic aerosol, are related 20 to iSOA, iSOA concentrations and O:C ratios from ECHAM-HAMMOZ are compared to atmospheric Atmospheric Mass Spectrometry (AMS) measurements from different field campaigns given in Table 6. Measurements were selected from AMS global database (Zhang et al., last accessed on 22.09.2017) according to the availability of elemental ratios. All campaigns took place either in Europe or North America and include six different countries. In Helsinki, Finland winter and spring measurements are available.



Location	Observation time period	Reference
Helsinki, Finland (60.2° N, 24.95° E)	08.01. - 14.03.2009 (W)	Carbone et al. (2014)
	09.04. - 08.05.2009 (S)	Timonen et al. (2010)
Mace Head, Ireland (53.33° N, 9.99° W)	25.02. - 26.03.2009	Dall'Osto et al. (2009)
Po Valley, Italy (44.65° N, 11.62° E)	31.03. - 20.04.2008	Saarikoski et al. (2012)
Houston, USA (29.8° N, 95.4° W)	15.08. - 15.09.2000	Zhang et al. (2007)
Mexico City, Mexico (19.48° N, 99.15° W)	10.03. - 30.03.2006	Aiken et al. (2009, 2010)
Manaus, Brazil (2.58° S, 60.2° W)	06.02. - 13.03.2008	Chen et al. (2009); Pöschl et al. (2010); Martin et al. (2010)

**Table 6.** Overview ambient measurement locations, time periods and references. For Helsinki there are two time series, one during winter (W) and the second during spring (S).

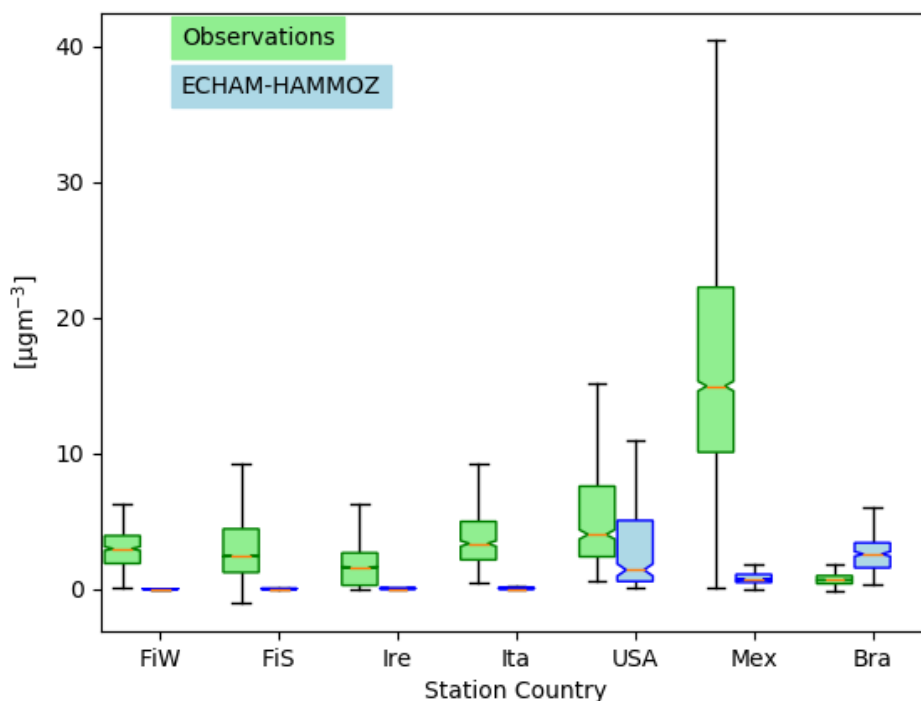


**Figure 8.** Box plots showing the variability of concentrations measured and corresponding instantaneous values from ECHAM-HAMMOZ. Countries of measurement campaigns are given. First, European countries then American ones. The shortcuts refer to: FiW=Helsinki, Finland (Winter), FiS=Helsinki, Finland (Spring), Ire=Mace Head, Ireland, Ita=Po Valley, Italy, USA=Houston Texas, USA, Mex=Mexico City, Mexico, Bra=Manaus, Brazil. The model time resolution is three hours, whereas all values given from the observations are included meaning that they have a higher time resolution.

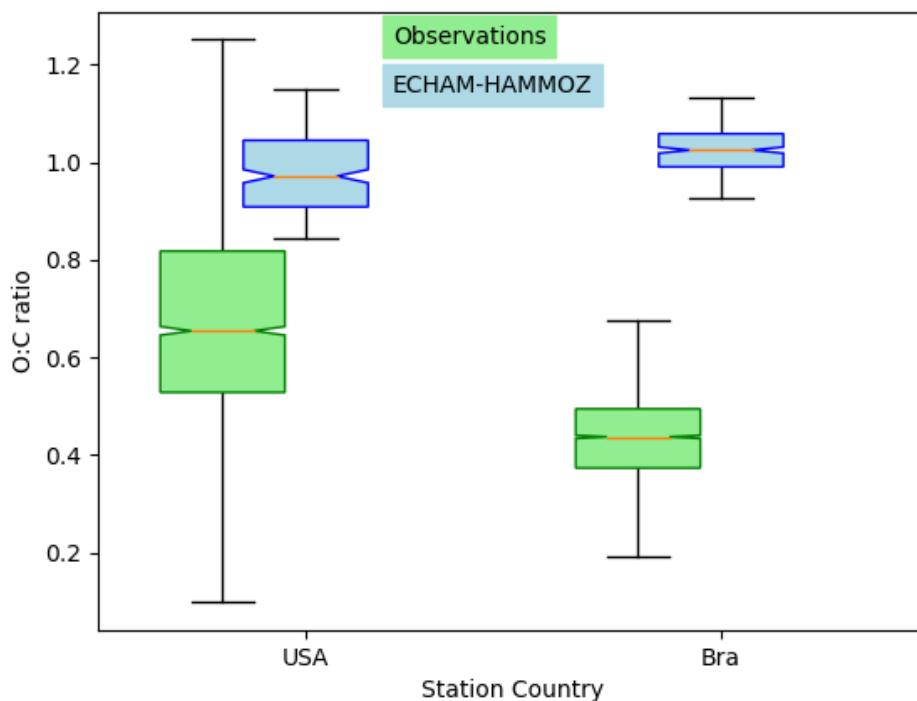


**Figure 9.** Similar to Figure 8 showing corresponding O:C ratios of the subset Houston Texas, USA and Manaus, Brazil. The O:C ratios shown here are corrected by the factor 1.27 according to Canagaratna et al. (2015)

Figure 8 shows the quartiles of the time series of the concentrations in the different locations, from left to right first the four European data sets and then the American ones. The European data sets display a variety of local OA sources. For Helsinki, Carbone et al. (2014) report a variety of local sources for OA including biomass burning, traffic, coffee roaster and also SOA from long range transport. In Mace Head two different OA types are measured depending on the advection of either marine air or continental air (Dall'Osto et al., 2009). Saarikoski et al. (2012) identified in Po Valley a complex mixture of OA with local and regional sources, mainly from anthropogenic origin. For Finland, Ireland and Italy, ECHAM-HAMMOZ reveals a minor contribution of iSOA to OA this can be explained by the measurement time periods in winter or early spring where vegetation in Europe does not emit large isoprene amounts (Steinbrecher et al., 2009).

Looking at the concentrations measured in Houston Texas, USA it can be seen that a great part of the variability is captured by iSOA, which is explained by high isoprene emissions found in Southeastern US. ECHAM-HAMMOZ median and percentiles are still lower than the observations since the observation includes total OA. The organic aerosol in Mexico City was measured at an urban super-site and covers such a big range of concentrations, which are dominated by anthropogenic emissions including biomass burning, nitrogen containing OA and primary hydrocarbon like OA associated with traffic (Aiken



et al., 2009). According to the concentrations simulated by ECHAM-HAMMOZ, just a minor part of these can be explained by iSOA. Manaus, Brazil is located in the Amazon Basin and classified as pristine environment close to pre-industrial conditions (Pöschl et al., 2010; Martin et al., 2010). Therefore, the particles are nearly pure biogenic and Martin et al. (2010) report an upper limit of 5% primary organic aerosol. These conditions are ideal to compare them to ECHAM-HAMMOZ just including  
5 iSOA, because isoprene emissions are high in the Amazon Basin and should dominate the OA there. As can be seen in Figure 8, HAMMOZ simulates overall higher iSOA concentrations than OA concentrations measured. Moreover, higher peak values are simulated and the median is higher than the upper 1.5 inter-quartile range whisker of observed concentrations.

For Houston Texas and Manaus, ECHAM-HAMMOZ relates a great part of the OA to iSOA, to further investigate this, O:C ratios are compared too. Due to restricted iSOA formation in ECHAM-HAMMOZ just from LVOC which are highly oxidized  
10 molecules with molecular O:C ratios between 0.6 and 1.4, the modeled O:C ratio just covers small variability and is around 1 in both regions, see Figure 9.

The comparison of concentration spectrum in Houston Texas showed a great part to be attributed to iSOA, this modeled subset covers upper values of the O:C ratio between 0.8 and 1.1, which still lie within the 75<sup>th</sup> percentile and the upper 1.5×IQR whisker of the measured data. This is related to the fact of missing SVOC and IVOC usually having lower O:C ratios  
15 and the contribution of POA to OA, which is not included in this comparison, because no assumptions of POA O:C ratios are made.

In contrast, the OA measured in Manaus located at the Amazon Basin, which consists of 95% SOA does not show as high O:C ratios as iSOA modeled by ECHAM-HAMMOZ. The median of observed aerosol lies at 0.4, instead of 1. Certainly part of it is explained by missing SVOC and IVOC in ECHAM-HAMMOZ, but might also be related to SOA from other organic  
20 molecules than isoprene. For Manaus an overestimation of iSOA concentrations by the model might be related to mistakes in emissions and in the chemical mechanism, missing sink processes and uncertainties in  $p^*$ . In term of O:C ratio of modeled iSOA between 0.6 and 1.4, the simulated values are covered by the ambient values in Houston Texas, but not in Manaus. This points to SVOC, IVOC and SOA from other sources than isoprene.

To summarize, isoprene emissions are not dominating OA in Europe, therefore the model shows iSOA having a small  
25 contribution to concentrations there. In contrast, American OA is more impacted by iSOA, especially in USA and Brazil.

#### 4 Discussion

The comparison of RefBase to the AeroCom models, ECHAM-HAM and AMS measurements in the isoprene dominated area Manaus in the Amazon basin revealed that semi-explicit treatment of atmospheric chemistry, at least for isoprene leads to much larger SOA production rates and eliminates low biases found in most other global model studies. In fact, especially over  
30 Brazil, SOA now has a tendency to be overestimated. This points to the possible importance of aerosol sink processes which have not been included in the current ECHAM-HAMMOZ version. Kroll et al. (2006) reported rapid chemical loss of SOA via photolysis could be a possibility to further transform iSOA either to higher oxidized molecules in the particle phase such as oligomers, or to fragment iSOA compounds leading to VOC and iSOA reduction. Hodzic et al. (2015) explored the global



impact of SOA photolysis and report about a 40 - 60% mass reduction after 10 days. SOA photolysis is closely related to wet-phase, in-particle chemistry, which is not included in the ECHAM-HAMMOZ chemical mechanism.

Extrapolating iSOA production rate to the production rate of SOA in ECHAM-HAMMOZ including SVOC, IVOC not only from isoprene, but also from terpenes and aromatics, we expect to find a portion of SOA which cannot be reduced by including the missing sinks known. Various reasons for this part of the overestimation of iSOA in ECHAM-HAMMOZ could be identified analyzing the results of the RefBase run and the several sensitivity runs.

First, overestimation of iSOA from isoprene derived LVOC already starts with the group contribution method used to estimate the saturation vapor pressure and evaporation enthalpy of these compounds. As discussed in O'Meara et al. (2014) and Barley and McFiggans (2010) the Nannoolal et al. (2008) method is problematic in the low volatility range, giving too low saturation pressures, which leads to an overestimation in SOA formation. Also comparing the logarithm of the saturation concentration at a reference temperature ( $\log_{10}C_0^*$ ) to the simple method of Donahue et al. (2011) reveals greatest differences in the lowest volatile compound LISOPOOHOOH pointing to the direction that the lowest volatile compound has most uncertain  $\log_{10}C_0^*$ . Since LISOPOOHOOH is high in ECHAM-HAMMOZ, it has great impact on iSOA. LISOPOOHOOH  $\log_{10}C_0^*$  might be higher and this would reduce the erroneous part of iSOA concentrations due to Nannoolal et al. (2008) method.

A second aspect leading to a high production in iSOA is the semi-explicit chemistry itself. Different chemical pathways lead to formation of isoprene LVOCs, some requiring NO and NO<sub>3</sub> for the initial steps followed OH, HO<sub>2</sub> or RO<sub>2</sub>. Formation of LVOCs via the NO<sub>x</sub>-depended pathway hardly happens, as can be seen in the chemical budget terms. LNISOOH and LC578OOH are formed in very low concentrations and C59OOH might just result from the HO<sub>2</sub>-dominated pathway. From the chemical branching it can be clearly seen that in JAM3 the OH initiated pathway is preferred, even in regions where NO mixing ratios are higher than 200 pptv (not shown). 90% of iSOA consist of products from this pathway, mostly IEPOX and LISOPOOHOOH. For LIEPOX this might lead to a large overestimation when acidic enhancement is considered. Highly acidic aerosol is expected in regions where sulfate pollution is high and these regions usually coincide with high NO<sub>x</sub>, which should suppress LIEPOX formation. In the atmosphere, both processes compensate each other, but in  $\gamma$ pH no NO<sub>x</sub>-suppression takes place, only acidic enhancement leading to high LIEPOX-SOA concentrations. Further, LISPOOHOOH production might be high due to missing intramolecular H-shift of LISOPOOHOOH which would lead to products with a saturation vapor pressure which is around 2 orders of magnitude higher than the one of LISOPOOHOOH (see Section 2.1.1, D'Ambro et al. (2017b)). Both processes as represented in ECHAM-HAMMOZ lead to an upper estimate of iSOA formation by these isoprene oxidation products.

Third, the main iSOA formation pathways follow from OH initiated reactions, which is the main oxidation pathway for isoprene. Nevertheless, analysis from Schultz et al. (submitted) shows that due to problems in tropical dynamics of ECHAM6, the tropical region is too wet leading to a higher production of OH radicals and therefore is more oxidative than the real atmosphere. Tropical regions are those, where most of isoprene is emitted. Thus, gas phase precursor formation might be overestimated already, which translates into an iSOA overestimation. Moreover, there simply might be a lack of understanding of SOA formation in tropical regions, Lin et al. (2012) also found an overestimation of their modeled SOA compared to



measurements of tropical forest sited and conclude that more measurements and model studies are needed to improve the formation mechanism in the tropics.

Finally, model limitations in aerosol and cloud processing did not allow to implement in-cloud iSOA formation. This is not only a potential additional source, but also an additional sink. ECHAM-HAMMOZ just includes wet scavenging based on solubility following Henry's law, but according to Cole-Filipiak et al. (2010) the IEPOX hydrolysis reactions at low pH values have life times comparable to wet deposition. Heterogeneous uptake of IEPOX in cloud droplets and rain would lead to a decrease in gas phase concentrations without resulting in iSOA, because it is lost immediately due to precipitation. This would lower iSOA from LIEPOX, which now has a substantial contribution to total iSOA.

## 5 Conclusions

For the first time, the semi-explicit chemical treatment of isoprene oxidation in the chemical mechanism of a global chemistry climate model was connected to explicit partitioning of individual low volatility species according to their chemical structures. The chemistry model MOZ includes a total of 779 reactions, where 147 reactions describe the isoprene oxidation. Isoprene oxidation in MOZ leads to LVOCs which are explicitly partitioned and followed in specific aerosol bins by HAM-SALSA. The partitioning is based on the saturation vapor pressure derived from the molecular structure of each single compound. Furthermore, also reactive uptake of isoprene derived glyoxal and IEPOX was considered.

These two iSOA formation pathways lead to an isoprene SOA yield of 16% relative to the primary oxidation of isoprene by OH, NO<sub>3</sub>, and ozone in 2012. It was identified that in ECHAM-HAMMOZ most iSOA is produced via the OH oxidation initiated pathway which leads to production of IEPOX and ISOP(OOH)<sub>2</sub>, a compound recently detected in experimental studies. Together modeled IEPOX and ISOP(OOH)<sub>2</sub> yield a fraction of 86% of total iSOA mass. In total 61 TgC iSOA are produced. IEPOX forms 24.4 TgC and ISOP(OOH)<sub>2</sub> 28.3 TgC. 59.1 TgC iSOA are lost due to wet deposition, which is the main sink for iSOA in ECHAM-HAMMOZ. For 2012 an average iSOA burden of 0.7 TgC is calculated. These values were compared to SOA budgets in AeroCom models. ECHAM-HAMMOZ simulates a higher production rate than all models used in this AeroCom study.

Moreover, this explicit model system enables process understanding and discussion. While exploring the influence of aerosol pH on IEPOX reactive uptake, enhancement of iSOA formation was found especially over Southeastern US while suppression could be observed over the Amazon basin.

Evaporation enthalpy used in previous model studies was compared to the explicitly derived evaporation enthalpy used in ECHAM-HAMMOZ. A huge difference could be found in Clausius-Clapeyron curves, which does not translate to a big impact on iSOA formation due to the fact that only LVOC were used.

Comparison of ECHAM-HAMMOZ iSOA concentrations to AMS measurements showed that ECHAM-HAMMOZ does not underestimate iSOA formation. On the contrary, in isoprene dominated regions like Brazil an iSOA overestimation could be observed which gives the possibility to explore novel SOA sinks, like in-particle decomposition or photolysis. Not lowering the production rate, but including additional sinks is the strategy proposed by Hodzic et al. (2016). They conclude that because



several SOA sinks are currently excluded from global models, these models are expected to overestimate SOA concentrations. Instead of the expected overestimation, an underestimation is found in the majority of global models. With our explicit model system connecting the aerosol bin scheme SALSA with the chemistry model MOZ in the frame of the global model ECHAM-HAMMOZ sufficient SOA is produced to be able to explore new sink processes.

- 5 *Code availability.* The ECHAM6.3-HAM2.3MOZ1.0 model code can be found at <https://redmine.hammoz.ethz.ch/projects/hammoz/wiki/Echam630-ham23-moz10>. After registration the code is available for download via the Apache Subversion system (SVN). All changes made according to SALSA and MOZ coupling can also be found there in the Finnish Meteorological Institute (FMI) branch. Please do not hesitate to ask the authors for support getting the code.

*Competing interests.* No competing interests are present.

- 10 *Acknowledgements.* ECHAM-HAMMOZ simulations were supported by the Forschungszentrum Jülich and performed at the Jülich Supercomputing Centre (2016). We also want to thank Q. Zhang, C. Parworth, M. Lechner, and J.L. Jimenez for facilitating the comparison with observations with their AMS global database. K. Tsigaridis is acknowledged for sending detailed results from the AeroCom model inter-comparison. Further, we acknowledge the authors involved in measuring organic aerosol in the different campaigns shown in this study.



## References

- Aiken, A., Salcedo, D., Cubison, M. J., Huffman, J., DeCarlo, P., Ulbrich, I. M., Docherty, K. S., Sueper, D., Kimmel, J., Worsnop, D. R., et al.: Mexico City aerosol analysis during MILAGRO using high resolution aerosol mass spectrometry at the urban supersite (T0)–Part 1: Fine particle composition and organic source apportionment, *Atmospheric Chemistry and Physics*, 9, 6633–6653, 2009.
- 5 Aiken, A., Foy, B. d., Wiedinmyer, C., DeCarlo, P., Ulbrich, I. M., Wehrl, M., Szidat, S., Prevot, A., Noda, J., Wacker, L., et al.: Mexico city aerosol analysis during MILAGRO using high resolution aerosol mass spectrometry at the urban supersite (T0)–Part 2: Analysis of the biomass burning contribution and the non-fossil carbon fraction, *Atmospheric chemistry and physics*, 10, 5315–5341, 2010.
- Athanasopoulou, E., Vogel, H., Vogel, B., Tsimpidi, A., Pandis, S. N., Knote, C., and Fountoukis, C.: Modeling the meteorological and chemical effects of secondary organic aerosols during an EUCAARI campaign, *Atmospheric Chemistry and Physics*, 13, 625, 2012.
- 10 Barley, M. and McFiggans, G.: The critical assessment of vapour pressure estimation methods for use in modelling the formation of atmospheric organic aerosol, *Atmospheric Chemistry and Physics*, 10, 749–767, 2010.
- Bergman, T., Kerminen, V.-M., Korhonen, H., Lehtinen, K., Makkonen, R., Arola, A., Mielonen, T., Romakkaniemi, S., Kulmala, M., and Kokkola, H.: Evaluation of the sectional aerosol microphysics module SALSA implementation in ECHAM5-HAM aerosol-climate model, *Geoscientific Model Development*, 5, 845–868, 2012.
- 15 Berndt, T., Herrmann, H., Sipilä, M., and Kulmala, M.: Highly Oxidized Second-Generation Products from the Gas-Phase Reaction of OH Radicals with Isoprene, *J. Phys. Chem. A*, 120, 10 150–10 159, 2016.
- Canagaratna, M., Jimenez, J., Kroll, J., Chen, Q., Kessler, S., Massoli, P., Hildebrandt Ruiz, L., Fortner, E., Williams, L., Wilson, K., et al.: Elemental ratio measurements of organic compounds using aerosol mass spectrometry: characterization, improved calibration, and implications, *Atmospheric Chemistry and Physics*, 15, 253–272, 2015.
- 20 Carbone, S., Aurela, M., Saarnio, K., Saarikoski, S., Timonen, H., Frey, A., Sueper, D., Ulbrich, I. M., Jimenez, J. L., Kulmala, M., et al.: Wintertime aerosol chemistry in sub-Arctic urban air, *Aerosol Science and Technology*, 48, 313–323, 2014.
- Chen, Q., Farmer, D., Schneider, J., Zorn, S., Heald, C., Karl, T., Guenther, A., Allan, J., Robinson, N., Coe, H., et al.: Mass spectral characterization of submicron biogenic organic particles in the Amazon Basin, *Geophysical Research Letters*, 36, 2009.
- Claeys, M., Graham, B., Vas, G., Wang, W., Vermeylen, R., Pashynska, V., Cafmeyer, J., Guyon, P., Andreae, M. O., Artaxo, P., et al.: 25 Formation of secondary organic aerosols through photooxidation of isoprene, *Science*, 303, 1173–1176, 2004.
- Clegg, S. L., Brimblecombe, P., and Wexler, A. S.: Thermodynamic Model of the System H<sup>+</sup>- NH<sub>4</sub><sup>+</sup>- Na<sup>+</sup>- SO<sub>4</sub><sup>2-</sup>- NO<sub>3</sub><sup>-</sup>- Cl<sup>-</sup>- H<sub>2</sub>O at 298.15 K, *The Journal of Physical Chemistry A*, 102, 2155–2171, 1998.
- Clements, A. L. and Seinfeld, J. H.: Detection and quantification of 2-methyltetrols in ambient aerosol in the southeastern United States, *Atmospheric Environment*, 41, 1825–1830, 2007.
- 30 Cole-Filipiak, N. C., O'Connor, A. E., and Elrod, M. J.: Kinetics of the hydrolysis of atmospherically relevant isoprene-derived hydroxy epoxides, *Environmental science & technology*, 44, 6718–6723, 2010.
- Dall'Osto, M., Ceburnis, D., Martucci, G., Bialek, J., Dupuy, R., Jennings, S., Berresheim, H., Wenger, J., Sodeau, J., Healy, R., et al.: Aerosol properties associated with air masses arriving into the North East Atlantic during the 2008 Mace Head EUCAARI intensive observing period: an overview., *Atmospheric Chemistry & Physics Discussions*, 9, 2009.
- 35 D'Ambro, E. L., Lee, B. H., Liu, J., Shilling, J. E., Gaston, C. J., Lopez-Hilfiker, F. D., Schobesberger, S., Zaveri, R. A., Mohr, C., Lutz, A., et al.: Molecular composition and volatility of isoprene photochemical oxidation secondary organic aerosol under low-and high-NO<sub>x</sub> conditions, *Atmospheric Chemistry and Physics*, 17, 159–174, 2017a.



- D'Ambro, E. L., Møller, K. H., Lopez-Hilfiker, F. D., Schobesberger, S., Liu, J., Shilling, J. E., Lee, B. H., Kjaergaard, H. G., and Thornton, J. A.: Isomerization of Second-Generation Isoprene Peroxy Radicals: Epoxide Formation and Implications for Secondary Organic Aerosol Yields, *Environmental Science & Technology*, 51, 4978–4987, 2017b.
- De Gouw, J. and Jimenez, J. L.: *Organic aerosols in the Earth's atmosphere*, 2009.
- 5 Dentener, F., Kinne, S., Bond, T., Boucher, O., Cofala, J., Generoso, S., Ginoux, P., Gong, S., Hoelzemann, J., Ito, A., et al.: Emissions of primary aerosol and precursor gases in the years 2000 and 1750 prescribed data-sets for AeroCom, *Atmospheric Chemistry and Physics*, 6, 4321–4344, 2006.
- Donahue, N., Robinson, A., Stanier, C., and Pandis, S.: Coupled partitioning, dilution, and chemical aging of semivolatile organics, *Environmental Science & Technology*, 40, 2635–2643, 2006.
- 10 Donahue, N. M., Robinson, A. L., and Pandis, S. N.: Atmospheric organic particulate matter: From smoke to secondary organic aerosol, *Atmospheric Environment*, 43, 94–106, 2009.
- Donahue, N. M., Epstein, S., Pandis, S. N., and Robinson, A. L.: A two-dimensional volatility basis set: 1. organic-aerosol mixing thermodynamics, *Atmospheric Chemistry and Physics*, 11, 3303–3318, 2011.
- Eddingsaas, N. C., VanderVelde, D. G., and Wennberg, P. O.: Kinetics and products of the acid-catalyzed ring-opening of atmospherically relevant butyl epoxy alcohols, *The Journal of Physical Chemistry A*, 114, 8106–8113, 2010.
- 15 Emmons, L., Walters, S., Hess, P., Lamarque, J.-F., Pfister, G., Fillmore, D., Granier, C., Guenther, A., Kinnison, D., Laepple, T., et al.: Description and evaluation of the Model for Ozone and Related chemical Tracers, version 4 (MOZART-4), *Geoscientific Model Development*, 3, 43–67, 2010.
- Epstein, S. A., Riipinen, I., and Donahue, N. M.: A semiempirical correlation between enthalpy of vaporization and saturation concentration for organic aerosol, *Environmental science & technology*, 44, 743–748, 2009.
- 20 Ervens, B. and Volkamer, R.: Glyoxal processing by aerosol multiphase chemistry: towards a kinetic modeling framework of secondary organic aerosol formation in aqueous particles, *Atmospheric Chemistry and Physics*, 10, 8219–8244, 2010.
- Farina, S. C., Adams, P. J., and Pandis, S. N.: Modeling global secondary organic aerosol formation and processing with the volatility basis set: Implications for anthropogenic secondary organic aerosol, *Journal of Geophysical Research: Atmospheres*, 115, 2010.
- 25 Fröhlich-Nowoisky, J., Kampf, C. J., Weber, B., Huffman, J. A., Pöhlker, C., Andreae, M. O., Lang-Yona, N., Burrows, S. M., Gunthe, S. S., Elbert, W., et al.: Bioaerosols in the Earth system: Climate, health, and ecosystem interactions, *Atmospheric Research*, 182, 346–376, 2016.
- Fu, T.-M., Jacob, D. J., Wittrock, F., Burrows, J. P., Vrekoussis, M., and Henze, D. K.: Global budgets of atmospheric glyoxal and methylglyoxal, and implications for formation of secondary organic aerosols, *Journal of geophysical research: atmospheres*, 113, 2008.
- 30 Fuzzi, S., Baltensperger, U., Carslaw, K., Decesari, S., Denier Van Der Gon, H., Facchini, M., Fowler, D., Koren, I., Langford, B., Lohmann, U., et al.: Particulate matter, air quality and climate: lessons learned and future needs, *Atmospheric chemistry and physics*, 15, 8217–8299, 2015.
- Gaston, C. J., Riedel, T. P., Zhang, Z., Gold, A., Surratt, J. D., and Thornton, J. A.: Reactive uptake of an isoprene-derived epoxydiol to submicron aerosol particles, *Environmental science & technology*, 48, 11 178–11 186, 2014.
- 35 Ghan, S. J. and Schwartz, S. E.: Aerosol properties and processes: A path from field and laboratory measurements to global climate models, *Bulletin of the American Meteorological Society*, 88, 1059–1083, 2007.
- Goldstein, A. H. and Galbally, I. E.: *Known and unexplored organic constituents in the earth's atmosphere*, 2007.



- Guenther, A., Karl, T., Harley, P., Wiedinmyer, C., Palmer, P., and Geron, C.: Estimates of global terrestrial isoprene emissions using MEGAN (Model of Emissions of Gases and Aerosols from Nature), *Atmospheric Chemistry and Physics Discussions*, 6, 107–173, 2006.
- Hallquist, M., Wenger, J., Baltensperger, U., Rudich, Y., Simpson, D., Claeys, M., Dommen, J., Donahue, N., George, C., Goldstein, A., et al.: The formation, properties and impact of secondary organic aerosol: current and emerging issues, *Atmospheric Chemistry and Physics*, 9, 5155–5236, 2009.
- 5 Heald, C. L., Jacob, D. J., Park, R. J., Russell, L. M., Huebert, B. J., Seinfeld, J. H., Liao, H., and Weber, R. J.: A large organic aerosol source in the free troposphere missing from current models, *Geophysical Research Letters*, 32, 2005.
- Henrot, A.-J., Stanelle, T., Schröder, S., Siegenthaler, C., Taraborrelli, D., and Schultz, M. G.: Implementation of the MEGAN (v2. 1) biogenic emission model in the ECHAM6-HAMMOZ chemistry climate model, *Geoscientific Model Development*, 10, 903, 2017.
- 10 Hodzic, A., Madronich, S., Kasibhatla, P., Tyndall, G., Aumont, B., Jimenez, J., Lee-Taylor, J., and Orlando, J.: Organic photolysis reactions in tropospheric aerosols: effect on secondary organic aerosol formation and lifetime, *Atmospheric Chemistry and Physics*, 15, 9253–9269, 2015.
- Hodzic, A., Kasibhatla, P. S., Jo, D. S., Cappa, C. D., Jimenez, J. L., Madronich, S., and Park, R. J.: Rethinking the global secondary organic aerosol (SOA) budget: stronger production, faster removal, shorter lifetime, *Atmospheric Chemistry and Physics*, 16, 7917–7941, 2016.
- 15 IPCC: Annex I: Atlas of Global and Regional Climate Projections, book section AI, pp. 1311–1394, Cambridge University Press, Cambridge, United Kingdom and New York, NY, USA, <https://doi.org/10.1017/CBO9781107415324.029>, [www.climatechange2013.org](http://www.climatechange2013.org), 2013.
- Jimenez, J., Canagaratna, M., Donahue, N., Prevot, A., Zhang, Q., Kroll, J. H., DeCarlo, P. F., Allan, J. D., Coe, H., Ng, N., et al.: Evolution of organic aerosols in the atmosphere, *Science*, 326, 1525–1529, 2009.
- Jülich Supercomputing Centre: JURECA: General-purpose supercomputer at Jülich Supercomputing Centre, *Journal of large-scale research facilities*, 2, <https://doi.org/10.17815/jlsrf-2-121>, <http://dx.doi.org/10.17815/jlsrf-2-121>, 2016.
- 20 Kanakidou, M., Seinfeld, J., Pandis, S., Barnes, I., Dentener, F., Facchini, M., Dingenen, R. V., Ervens, B., Nenes, A., Nielsen, C., et al.: Organic aerosol and global climate modelling: a review, *Atmospheric Chemistry and Physics*, 5, 1053–1123, 2005.
- Kavouras, I. G., Mihalopoulos, N., and Stephanou, E. G.: Secondary organic aerosol formation vs primary organic aerosol emission: In situ evidence for the chemical coupling between monoterpene acidic photooxidation products and new particle formation over forests, *Environmental science & technology*, 33, 1028–1037, 1999.
- 25 Kinnison, D., Brasseur, G., Walters, S., Garcia, R., Marsh, D., Sassi, F., Harvey, V., Randall, C., Emmons, L., Lamarque, J., et al.: Sensitivity of chemical tracers to meteorological parameters in the MOZART-3 chemical transport model, *Journal of Geophysical Research: Atmospheres* (1984–2012), 112, 2007.
- Kokkola, H., Korhonen, H., Lehtinen, K., Makkonen, R., Asmi, A., Järvenoja, S., Anttila, T., Partanen, A.-I., Kulmala, M., Järvinen, H., et al.: SALSAs—a Sectional Aerosol module for Large Scale Applications, *Atmospheric Chemistry and Physics*, 8, 2469–2483, 2008.
- 30 Kourtchev, I., Ruuskanen, T., Maenhaut, W., Kulmala, M., and Claeys, M.: Observation of 2-methyltetrols and related photo-oxidation products of isoprene in boreal forest aerosols from Hyytiälä, Finland, *Atmospheric Chemistry and Physics*, 5, 2761–2770, 2005.
- Kroll, J. H., Ng, N. L., Murphy, S. M., Flagan, R. C., and Seinfeld, J. H.: Secondary organic aerosol formation from isoprene photooxidation, *Environmental science & technology*, 40, 1869–1877, 2006.
- 35 Kühn, T., Merikanto, J., Mielonen, T., Stadtler, S., Hienola, A., Korhonen, H., Ferrachat, S., Lohmann, U., Neubauer, D., Tegen, I., Siegenthaler-Le Drian, C., Wahl, S., Schultz, M. G., Rast, S., Schmidt, H., Stier, P., Lehtinen, K., and Kokkola, H.: SALSAs2.0 part2: Implementation of a volatility basis set to model formation of secondary organic aerosol, in preparation.



- Lakey, P. S., Berkemeier, T., Tong, H., Arangio, A. M., Lucas, K., Pöschl, U., and Shiraiwa, M.: Chemical exposure-response relationship between air pollutants and reactive oxygen species in the human respiratory tract, *Scientific reports*, 6, 32916, 2016.
- Lal, V., Khalizov, A. F., Lin, Y., Galvan, M. D., Connell, B. T., and Zhang, R.: Heterogeneous reactions of epoxides in acidic media, *The Journal of Physical Chemistry A*, 116, 6078–6090, 2012.
- 5 Lamarque, J.-F., Bond, T. C., Eyring, V., Granier, C., Heil, A., Klimont, Z., Lee, D., Liou, S. C., Mieville, A., Owen, B., et al.: Historical (1850–2000) gridded anthropogenic and biomass burning emissions of reactive gases and aerosols: methodology and application, *Atmospheric Chemistry and Physics*, 10, 7017–7039, 2010.
- Lelieveld, J., Gromov, S., Pozzer, A., and Taraborrelli, D.: Global tropospheric hydroxyl distribution, budget and reactivity, *Atmos. Chem. Phys.*, 16, 12477–12493, 2016.
- 10 Li, N., Fu, T.-M., Cao, J., Lee, S., Huang, X.-F., He, L.-Y., Ho, K.-F., Fu, J. S., and Lam, Y.-F.: Sources of secondary organic aerosols in the Pearl River Delta region in fall: Contributions from the aqueous reactive uptake of dicarbonyls, *Atmospheric environment*, 76, 200–207, 2013.
- Liggio, J., Li, S.-M., and McLaren, R.: Heterogeneous reactions of glyoxal on particulate matter: Identification of acetals and sulfate esters, *Environmental science & technology*, 39, 1532–1541, 2005a.
- 15 Liggio, J., Li, S.-M., and McLaren, R.: Reactive uptake of glyoxal by particulate matter, *Journal of Geophysical Research: Atmospheres*, 110, 2005b.
- Lin, G., Penner, J., Sillman, S., Taraborrelli, D., and Lelieveld, J.: Global modeling of SOA formation from dicarbonyls, epoxides, organic nitrates and peroxides, *Atmospheric Chemistry and Physics*, 12, 4743–4774, 2012.
- Lin, S.-J. and Rood, R. B.: Multidimensional flux-form semi-Lagrangian transport schemes, *Monthly Weather Review*, 124, 2046–2070, 20
- 1996.
- Lin, Y.-H., Knipping, E., Edgerton, E., Shaw, S., and Surratt, J.: Investigating the influences of SO<sub>2</sub> and NH<sub>3</sub> levels on isoprene-derived secondary organic aerosol formation using conditional sampling approaches, *Atmospheric Chemistry and Physics*, 13, 8457–8470, 2013a.
- Lin, Y.-H., Zhang, H., Pye, H. O., Zhang, Z., Marth, W. J., Park, S., Arashiro, M., Cui, T., Budisulistiorini, S. H., Sexton, K. G., et al.: Epoxide as a precursor to secondary organic aerosol formation from isoprene photooxidation in the presence of nitrogen oxides, *Proceedings of the National Academy of Sciences*, 110, 6718–6723, 2013b.
- 25 Liu, J., D'Ambro, E. L., Lee, B. H., Lopez-Hilfiker, F. D., Zaveri, R. A., Rivera-Rios, J. C., Keutsch, F. N., Iyer, S., Kurten, T., Zhang, Z., et al.: Efficient isoprene secondary organic aerosol formation from a non-IEPOX pathway, *Environmental science & technology*, 50, 9872–9880, 2016.
- Lopez-Hilfiker, F., Mohr, C., D'Ambro, E. L., Lutz, A., Riedel, T. P., Gaston, C. J., Iyer, S., Zhang, Z., Gold, A., Surratt, J. D., et al.: 30 Molecular composition and volatility of organic aerosol in the Southeastern US: implications for IEPOX derived SOA, *Environmental science & technology*, 50, 2200–2209, 2016.
- Marais, E. A., Jacob, D. J., Jimenez, J. L., Campuzano-Jost, P., Day, D. A., Hu, W., Krechmer, J., Zhu, L., Kim, P. S., Miller, C. C., et al.: Aqueous-phase mechanism for secondary organic aerosol formation from isoprene: application to the southeast United States and co-benefit of SO<sub>2</sub> emission controls, *Atmospheric Chemistry and Physics*, 16, 1603–1618, 2016.
- 35 Martin, S., Andreae, M., Althausen, D., Artaxo, P., Baars, H., Borrmann, S., Chen, Q., Farmer, D., Guenther, A., Gunthe, S., et al.: An overview of the Amazonian aerosol characterization experiment 2008 (AMAZE-08), *Atmospheric Chemistry and Physics*, 10, 2010.



- McFiggans, G., Topping, D., and Barley, M.: The sensitivity of secondary organic aerosol component partitioning to the predictions of component properties—Part 1: A systematic evaluation of some available estimation techniques, *Atmospheric Chemistry and Physics*, 10, 10 255–10 272, 2010.
- McNeill, V. F., Woo, J. L., Kim, D. D., Schwier, A. N., Wannell, N. J., Sumner, A. J., and Barakat, J. M.: Aqueous-phase secondary organic aerosol and organosulfate formation in atmospheric aerosols: a modeling study, *Environmental science & technology*, 46, 8075–8081, 2012.
- Nannoolal, Y., Rarey, J., Ramjugernath, D., and Cordes, W.: Estimation of pure component properties: Part 1. Estimation of the normal boiling point of non-electrolyte organic compounds via group contributions and group interactions, *Fluid Phase Equilibria*, 226, 45–63, 2004.
- 10 Nannoolal, Y., Rarey, J., and Ramjugernath, D.: Estimation of pure component properties: Part 3. Estimation of the vapor pressure of non-electrolyte organic compounds via group contributions and group interactions, *Fluid Phase Equilibria*, 269, 117–133, 2008.
- Nölscher, A., Butler, T., Auld, J., Veres, P., Muñoz, A., Taraborrelli, D., Vereecken, L., Lelieveld, J., and Williams, J.: Using total OH reactivity to assess isoprene photooxidation via measurement and model, *Atmospheric Environment*, 89, 453–463, 2014.
- Nozière, B., González, N. J., Borg-Karlson, A.-K., Pei, Y., Redeby, J. P., Krejci, R., Dommen, J., Prevot, A. S., and Anthonsen, T.: Atmospheric chemistry in stereo: A new look at secondary organic aerosols from isoprene, *Geophysical Research Letters*, 38, 2011.
- ODonnell, D., Tsigaridis, K., and Feichter, J.: Estimating the direct and indirect effects of secondary organic aerosols using ECHAM5-HAM, *Atmospheric Chemistry and Physics*, 11, 8635–8659, 2011.
- Odum, J. R., Hoffmann, T., Bowman, F., Collins, D., Flagan, R. C., and Seinfeld, J. H.: Gas/particle partitioning and secondary organic aerosol yields, *Environmental Science & Technology*, 30, 2580–2585, 1996.
- 20 OMeara, S., Booth, A. M., Barley, M. H., Topping, D., and McFiggans, G.: An assessment of vapour pressure estimation methods, *Physical Chemistry Chemical Physics*, 16, 19 453–19 469, 2014.
- Pandis, S. N., Harley, R. A., Cass, G. R., and Seinfeld, J. H.: Secondary organic aerosol formation and transport, *Atmospheric Environment. Part A. General Topics*, 26, 2269–2282, 1992.
- Pankow, J. F.: An absorption model of gas/particle partitioning of organic compounds in the atmosphere, *Atmospheric Environment*, 28, 25 185–188, 1994.
- Paulot, F., Crounse, J. D., Kjaergaard, H. G., Kürten, A., Clair, J. M. S., Seinfeld, J. H., and Wennberg, P. O.: Unexpected epoxide formation in the gas-phase photooxidation of isoprene, *Science*, 325, 730–733, 2009.
- Pöschl, U., Martin, S., Sinha, B., Chen, Q., Gunthe, S., Huffman, J., Borrmann, S., Farmer, D., Garland, R., Helas, G., et al.: Rainforest aerosols as biogenic nuclei of clouds and precipitation in the Amazon, *science*, 329, 1513–1516, 2010.
- 30 Pye, H. O., Pinder, R. W., Piletic, I. R., Xie, Y., Capps, S. L., Lin, Y.-H., Surratt, J. D., Zhang, Z., Gold, A., Luecken, D. J., et al.: Epoxide pathways improve model predictions of isoprene markers and reveal key role of acidity in aerosol formation, *Environmental science & technology*, 47, 11 056–11 064, 2013.
- Riedel, T. P., Lin, Y.-H., Budisulistiorini, S. H., Gaston, C. J., Thornton, J. A., Zhang, Z., Vizuete, W., Gold, A., and Surratt, J. D.: Heterogeneous reactions of isoprene-derived epoxides: reaction probabilities and molar secondary organic aerosol yield estimates, *Environmental Science & Technology Letters*, 2, 38–42, 2015.
- 35 Riva, M., Budisulistiorini, S. H., Chen, Y., Zhang, Z., D'Ambro, E. L., Zhang, X., Gold, A., Turpin, B. J., Thornton, J. A., Canagaratna, M. R., et al.: Chemical characterization of secondary organic aerosol from oxidation of isoprene hydroxyhydroperoxides, *Environmental science & technology*, 50, 9889–9899, 2016.



- Saarikoski, S., Carbone, S., Decesari, S., Giulianelli, L., Angelini, F., Canagaratna, M., Ng, N., Trimborn, A., Facchini, M., Fuzzi, S., et al.: Chemical characterization of springtime submicrometer aerosol in Po Valley, Italy, *Atmospheric Chemistry and Physics*, 12, 8401–8421, 2012.
- Schultz, M. G., Stadtler, S., Schroeder, S., Taraborrelli, D., Henrot, A., Kaffashzadeh, N., Franco, B., Ferrachat, S., Siegenthaler-Le Drian, C., Lohmann, U., Neubauer, D., Wahl, S., Kokkola, H., Kuehn, T., Stier, P., Kinnison, D., Tyndall, G., and Orlando, J.: The Chemistry Climate Model ECHAM-HAMMOZ, *Global Model Development*, submitted.
- Schwartz, S. E.: Mass-transport considerations pertinent to aqueous phase reactions of gases in liquid-water clouds, in: *Chemistry of multi-phase atmospheric systems*, pp. 415–471, Springer, 1986.
- Seinfeld, J. H. and Pankow, J. F.: Organic atmospheric particulate material, *Annual review of physical chemistry*, 54, 121–140, 2003.
- 10 Shiraiwa, M., Li, Y., Tsimpidi, A. P., Karydis, V. A., Berkemeier, T., Pandis, S. N., Lelieveld, J., Koop, T., and Pöschl, U.: Global distribution of particle phase state in atmospheric secondary organic aerosols, *Nature communications*, 8, 2017.
- Stadtler, S., Simpson, D., Schröder, S., Taraborrelli, D., Bott, A., and Schultz, M.: Ozone Impacts of Gas-Aerosol Uptake in Global Chemistry Transport Models, *Atmos. Chem. Phys.*, 2017.
- Stein, O., Flemming, J., Inness, A., Kaiser, J. W., and Schultz, M. G.: Global reactive gases forecasts and reanalysis in the MACC project, 15 *Journal of Integrative Environmental Sciences*, 9, 57–70, 2012.
- Steinbrecher, R., Smiatek, G., Köble, R., Seufert, G., Theloke, J., Hauß, K., Ciccioli, P., Vautard, R., and Curci, G.: Intra- and inter-annual variability of VOC emissions from natural and semi-natural vegetation in Europe and neighbouring countries, *Atmospheric Environment*, 43, 1380–1391, 2009.
- Stevens, B., Giorgetta, M., Esch, M., Mauritsen, T., Crueger, T., Rast, S., Salzmann, M., Schmidt, H., Bader, J., Block, K., et al.: Atmospheric 20 component of the MPI-M Earth System Model: ECHAM6, *Journal of Advances in Modeling Earth Systems*, 5, 146–172, 2013.
- Stier, P., Feichter, J., Kinne, S., Kloster, S., Vignati, E., Wilson, J., Ganzeveld, L., Tegen, I., Werner, M., Balkanski, Y., et al.: The aerosol-climate model ECHAM5-HAM, *Atmospheric Chemistry and Physics*, 5, 1125–1156, 2005.
- Surratt, J. D., Murphy, S. M., Kroll, J. H., Ng, N. L., Hildebrandt, L., Sorooshian, A., Szmigielski, R., Vermeylen, R., Maenhaut, W., Claeys, M., et al.: Chemical composition of secondary organic aerosol formed from the photooxidation of isoprene, *The Journal of Physical 25 Chemistry A*, 110, 9665–9690, 2006.
- Surratt, J. D., Kroll, J. H., Kleindienst, T. E., Edney, E. O., Claeys, M., Sorooshian, A., Ng, N. L., Offenberg, J. H., Lewandowski, M., Jaoui, M., et al.: Evidence for organosulfates in secondary organic aerosol, *Environmental Science & Technology*, 41, 517–527, 2007a.
- Surratt, J. D., Lewandowski, M., Offenberg, J. H., Jaoui, M., Kleindienst, T. E., Edney, E. O., and Seinfeld, J. H.: Effect of acidity on secondary organic aerosol formation from isoprene, *Environmental Science & Technology*, 41, 5363–5369, 2007b.
- 30 Surratt, J. D., Chan, A. W., Eddingsaas, N. C., Chan, M., Loza, C. L., Kwan, A. J., Hersey, S. P., Flagan, R. C., Wennberg, P. O., and Seinfeld, J. H.: Reactive intermediates revealed in secondary organic aerosol formation from isoprene, *Proceedings of the National Academy of Sciences*, 107, 6640–6645, 2010.
- Taraborrelli, D., Lawrence, M., Butler, T., Sander, R., and Lelieveld, J.: Mainz Isoprene Mechanism 2 (MIM2): an isoprene oxidation mechanism for regional and global atmospheric modelling, *Atmospheric Chemistry and Physics*, 9, 2751–2777, 2009.
- 35 Taraborrelli, D., Lawrence, M., Crowley, J., Dillon, T., Gromov, S., Groß, C., Vereecken, L., and Lelieveld, J.: Hydroxyl radical buffered by isoprene oxidation over tropical forests, *Nature Geoscience*, 5, 190, 2012.



- Timonen, H., Aurela, M., Carbone, S., Saarnio, K., Saarikoski, S., Mäkelä, T., Kulmala, M., Kerminen, V.-M., Worsnop, D., and Hillamo, R.: High time-resolution chemical characterization of the water-soluble fraction of ambient aerosols with PILS-TOC-IC and AMS, *Atmospheric Measurement Techniques*, 3, 1063–1074, 2010.
- 5 Topping, D., Barley, M., Bane, M., Higham, N. J., Aumont, B., Dingle, N., and McFiggans, G.: UManSysProp v1. 0: an online and open-source facility for molecular property prediction and atmospheric aerosol calculations, *Geosci. Model. Dev.*, 9, 899–914, <https://doi.org/https://doi.org/10.5194/gmd-9-899-2016>, 2016.
- Tsigaridis, K. and Kanakidou, M.: Global modelling of secondary organic aerosol in the troposphere: a sensitivity analysis, *Atmospheric Chemistry and Physics*, 3, 1849–1869, 2003.
- 10 Tsigaridis, K., Daskalakis, N., Kanakidou, M., Adams, P., Artaxo, P., Bahadur, R., Balkanski, Y., Bauer, S., Bellouin, N., Benedetti, A., et al.: The AeroCom evaluation and intercomparison of organic aerosol in global models, *Atmospheric Chemistry and Physics*, 14, 10 845–10 895, 2014.
- Volkamer, R., Jimenez, J. L., San Martini, F., Dzepina, K., Zhang, Q., Salcedo, D., Molina, L. T., Worsnop, D. R., and Molina, M. J.: Secondary organic aerosol formation from anthropogenic air pollution: Rapid and higher than expected, *Geophysical Research Letters*, 33, 2006.
- 15 Volkamer, R., San Martini, F., Molina, L. T., Salcedo, D., Jimenez, J. L., and Molina, M. J.: A missing sink for gas-phase glyoxal in Mexico City: Formation of secondary organic aerosol, *Geophysical Research Letters*, 34, 2007.
- Washenfelder, R., Young, C., Brown, S., Angevine, W., Atlas, E., Blake, D., Bon, D., Cubison, M., De Gouw, J., Dusanter, S., et al.: The glyoxal budget and its contribution to organic aerosol for Los Angeles, California, during CalNex 2010, *Journal of Geophysical Research: Atmospheres*, 116, 2011.
- 20 Waxman, E. M., Dzepina, K., Ervens, B., Lee-Taylor, J., Aumont, B., Jimenez, J. L., Madronich, S., and Volkamer, R.: Secondary organic aerosol formation from semi- and intermediate-volatility organic compounds and glyoxal: Relevance of O/C as a tracer for aqueous multiphase chemistry, *Geophysical Research Letters*, 40, 978–982, 2013.
- Woo, J. and McNeill, V.: simpleGAMMA v1. 0—a reduced model of secondary organic aerosol formation in the aqueous aerosol phase (aaSOA), *Geoscientific Model Development*, 8, 1821–1829, 2015.
- 25 Xu, L., Guo, H., Boyd, C. M., Klein, M., Bougiatioti, A., Cerully, K. M., Hite, J. R., Isaacman-VanWertz, G., Kreisberg, N. M., Knote, C., et al.: Effects of anthropogenic emissions on aerosol formation from isoprene and monoterpenes in the southeastern United States, *Proceedings of the National Academy of Sciences*, 112, 37–42, 2015.
- Zhang, Q., Jimenez, J., Canagaratna, M., Allan, J., Coe, H., Ulbrich, I., Alfarra, M., Takami, A., Middlebrook, A., Sun, Y., et al.: Ubiquity and dominance of oxygenated species in organic aerosols in anthropogenically-influenced Northern Hemisphere midlatitudes, *Geophysical*
- 30 *Research Letters*, 34, 2007.
- Zhang, Q., Parworth, C., Lechner, M., and Jimenez, J.: Aerosol Mass Spectrometer Global Database, <https://doi.org/doi:10.6084/m9.figshare.3486719>, <https://sites.google.com/site/amsglobaldatabase>, last accessed on 22.09.2017.